Distribution of *n*-alkanes and their δ^2H and $\delta^{13}C$ values in typical plants along a terrestrial-coastal-oceanic gradient

Ding He [a, b, c*], S. Nemiah Ladd [d, e,1], Colin J. Saunders [f], Ralph N. Mead [g], Rudolf Jaffé [c]

[a] *Key Laboratory of Geoscience Big Data and Deep Resource of Zhejiang Province, School of Earth Sciences, Zhejiang University, Hangzhou, China*

[b] *State Key Laboratory of Satellite Ocean Environment Dynamics, Second Institute of Oceanography, Ministry of Natural Resources, Hangzhou, China*

[c] *Southeast Environmental Research Center and Department of Chemistry and Biochemistry, Florida International University, 3000 NE 151st St., North Miami, FL, USA*

[d] *Department of Surface Waters – Research and Management, Swiss Federal Institute of Aquatic Science and Technology (Eawag), Seestrasse 79, Kastanienbaum, Switzerland*

[e] *Department of Earth Sciences, ETH-Zürich, Sonneggstrasse 5, Zürich, Switzerland*

[f] *South Florida Water Management District, West Palm Beach, FL, USA*

[g] *Department of Chemistry and Biochemistry, University of North Carolina Wilmington, Wilmington, NC, USA*

[1] *Current address: Ecosystem Physiology, University of Freiburg, 53/54 Georges-Köhler Allee, 79110 Freiburg, Germany*

Corresponding at D. He, email address: dinghe@zju.edu.cn

ABSTRACT

Reconstructing past responses of coastal wetlands to climate change contextualizes ongoing and future developments in these globally important ecosystems. The molecular distributions and stable isotope ratios (δ^2H and $\delta^{13}C$) of sedimentary plant wax *n*-alkanes are frequently used to infer past vegetation and hydroclimate changes in wetland systems. However, there is limited modern information available about these compounds in subtropical wetlands. Here we analyzed mature leaves from 30 typical plant species and roots from 6 plant species collected in the Florida Everglades, including

This document is the accepted manuscript version of the following article:
He, D., Nemiah Ladd, S., Saunders, C. J., Mead, R. N., & Jaffé, R. (2020). Distribution of n-alkanes and their δ2H and δ13C values in typical plants along a terrestrial-coastal-oceanic gradient. Geochimica et Cosmochimica Acta, 281, 31-52.
https://doi.org/10.1016/j.gca.2020.05.003

tree island plants, freshwater wetland plants, mangroves, and seagrass. The *n*-alkane abundance (2 to 884 μg/g dry weight), percent of aquatic plants ratio (P*aq*, 0 to 1), average chain length ($ACL_{23\text{-}33}$, 24.0 to 30.7), concentration weighted average (CWA) δ^2H (-231 to -78‰) and $\delta^{13}C$ values (-38.9 to -14.4‰) spanned wide ranges with plant growth habit. Significant differences in *n*-alkane abundances, P*aq*, $ACL_{23\text{-}33}$, CWA δ^2H and $\delta^{13}C$ values were found to exist between the leaves and roots of some emergent aquatic plants. Simple mass balance calculations of wetland aquatic plants suggest that long chain *n*-alkanes (e.g., C_{29} *n*-alkanes) are predominantly derived from leaves rather than roots in wetland surface sediments/soils. However, the contribution from mid-chain *n*-alkanes (e.g., C_{23} *n*-alkane) from roots may be equal to or greater than those from leaves. This implies that the differences in the isotopic compositions between root and leaf derived material need to be taken into account when interpreting down core changes in mid-chain *n*-alkane δ^2H and $d^{13}C$ values, which may be derived from variable contributions from leaves and roots rather than a change in hydroclimate or vegetation. Considering the large variation in both *n*-alkane distribution proxies and isotopic composition, no single molecular index or stable isotope ratio can capture multivariate changes of wetland ecosystems in the past. Nevertheless, principal component analysis shows promising potential to resolve different plant functional types. Paleo-reconstruction of subtropical aquatic ecosystems using *n*-alkanes will be most useful if the full molecular and isotopic distribution information of plant waxes are used.

Key words: *n*-Alkanes; Hydrogen isotopes; Carbon isotopes; Leaf; Root; Wetland; Paleo-reconstruction.

Highlights:

- Abundances, δ^2H and $\delta^{13}C$ values of *n*-alkanes were measured from plants across a coastal wetland.
- Most of the geochemical proxies differed among plant habitats and between leaves and roots.

- Differences in the isotopic values are larger among plants than between the leaves and roots.
- PCA is a valuable tool differentiating organic matter source in coastal wetland sediments.

1. Introduction:

The Florida Everglades is the largest sub-tropical coastal wetland system in North America. Since the early 20th century, Everglades wetlands have been significantly drained and structurally modified for flood control, urban development and agriculture. Drainage of the wetlands during the second half of the 20^{th} century resulted in diminished size, shifts in the composition and distribution of vegetation cover, loss of ridge and slough features in the landscape, and a decline in water quality (Davis et al., 1994). To design restoration plans that reverse or mitigate these changes and to better predict effects to future environmental changes, it is essential to have a better understanding of how historical changes have affected this ecosystem. Multi-proxy approaches are needed in order to provide robust and comprehensive historical environmental information.

Among various tools used in paleo-reconstruction, the molecular distributions and isotopic composition of leaf wax compounds (in particular mid and long-chain *n*-alkanes) are widely applied to reconstruct changes in sources of organic matter (e.g., Meyers, 1997; Hinrichs et al., 1999; Eglinton and Eglinton, 2008 and references therein), shifts in vegetation type (e.g., Ficken et al., 2000; Bi et al., 2005; He et al., 2016a), and climate variables including changes in precipitation, relative humidity, temperature and salinity (e.g., Xie et al., 2000; Liu and Huang, 2005; Tierney et al., 2008; Nelson and Sachs, 2016). However, the application of leaf wax biomarkers is limited in wetland ecosystems such as the Everglades because most of the calibration work to date has been focused on terrestrial plants (e.g., Sachse et al., 2012; Bush and McInerney, 2013; Diefendorf and Freimuth, 2017), and thus cannot necessarily be applied to aquatic systems. Therefore, the molecular and isotopic compositions of plant waxes along wetland vegetation gradients need to be assessed in modern ecosystems to determine their suitability as proxies for paleo-hydrology and ecology in wetland ecosystems.

Despite the enormous potential that leaf wax *n*-alkanes have as proxies of past climate and hydrology, various critical mechanisms responsible for their sedimentary distributions and isotopic concentrations remain unclear (Sachse et al., 2012; Bush and McInerney, 2013; Sessions, 2016; Diefendorf and Freimuth, 2017). One of the dominant causes of uncertainty is our limited understanding of the critical drivers that influence hydrogen and carbon isotope ratios of modern plants. First, *n*-alkane-δ^2H studies are based on the observation that the community-averaged $^2H/^1H$ fractionation is relatively stable, making leaf wax δ^2H values effective tracers of source water isotopes (e.g., Sachse et al., 2012), even though individual plant taxa growing at the same site have been observed to display dramatically different leaf water ^2H-fractionation factors during the biosynthesis of *n*-alkanes (Feakins and Sessions, 2010; Eley et al., 2014; Ladd and Sachs, 2015; Nelson et al., 2018). Moreover, several studies have noticed temporal scale variation of fractionation factors for the same species (e.g., Tipple et al., 2013; Freimuth et al., 2017; Tipple and Ehleringer, 2018).

While the positive correlation between the *n*-alkane δ^2H values of modern plant leaf wax and precipitation δ^2H values at global scales is robust (Sachse et al., 2012; McFarlin et al., 2019), setting up the foundation for paleo-reconstructions, the fact that sedimentary *n*-alkanes are likely derived from a variety of known and unknown sources leads to additional limitations for this proxy. In addition, these sources can (and likely do) change over time through geologic records as climate changes. Leaf waxes from trees, shrubs and grasses are generally assumed as the dominant source of wax delivered to soils or sediments (e.g., Gamarra and Kahmen, 2015; Diefendorf and Freimuth, 2017). In contrast, contributions from below ground biomass (including roots) have not been explicitly considered (Gocke et al., 2010; Mendez-Millan et al., 2010; Huang et al., 2011; Jansen and Wiesenberg, 2017), although increasing evidence suggests that the root biomass may also be an important source of organic matter (OM) in soils and sediments (Busch et al., 2004; Poret et al., 2007; Jansen and Wisenberg, 2017). Root biomass is especially important to consider in wetlands, where plants can develop shallow but flourishing root systems such as rootlets (Rydin and Jeglum, 2013) with high turnover rates (~55% per year, Gill and Jackson, 2000). In contrast to deeper lake or ocean sediments, where the presence of root-derived OM is limited by transport from eroded soils, in wetlands root-

118 derived OM will primarily remain in place and become effectively incorporated into the
119 soil record, competing with leaf litter fall as an important source of plant carbon to soils
120 (Fahey et al., 2005). Root-derived OM can contribute >70% of total plant-derived OM in
121 soils, and the mean residence time in soils of root-derived C is estimated as 2.4 times that
122 of shoot-derived C (Rasse et al., 2005). Such findings suggest the need to further
123 investigate wax (including *n*-alkanes) abundances and composition in plant roots (Huang
124 et al., 2011). Some studies have indicated that plant roots contain *n*-alkanes, including
125 long chain homologues (Jansen et al., 2006; Wiesenberg et al., 2010; Gamarra and
126 Kahmen, 2015). However, limited studies have performed detailed comparisons of the
127 molecular and the isotopic composition of wetland plants between leaves and roots.
128 Non-photosynthetic C_3 plant tissues generally are ^{13}C enriched compared with
129 leaves (Cernusak et al., 2009). Likewise, bulk root material is typically enriched in ^{2}H
130 relative to photosynthetic plant tissue (Ziegler et al., 1976). Only two pioneer studies
131 have investigated *n*-alkane $\delta^{2}H$ values between leaf and root materials, including a study
132 of 15 species of C3 grasses in an alpine and a temperate grassland of Switzerland
133 (Gamarra and Kahmen, 2015), and in a study of two grasses and a shrub species in the
134 Chinese Loess Plateau (Liu et al., 2019). The mean $\delta^{2}H$ values of leaf-derived *n*-alkanes
135 were in general more depleted than those of roots for all 18 species surveyed (except for
136 the *Stipa bungeana* (grass) and *Artemisisa vestita* (shrub)) in the Chinese Loess Plateau
137 (Gamarra and Kahmen, 2015; Liu et al., 2019). The different biochemical hydrogen
138 isotope fractionations, changes in the plant's carbon metabolism and hydrogen sources of
139 NADPH are likely the potential causes (Cormier et al., 2018). However, previous studies
140 all focused on terrestrial plants, and no such isotopic information between leaf and root
141 has ever been obtained for aquatic plants (i.e., submerged vs. emergent). This limits our
142 potential in the interpretation of *n*-alkane isotopic values for paleo-reconstruction in
143 aquatic ecosystems, where the contribution from roots could likely be significant.
144 A third limitation is that different plants have been reported to produce
145 significantly different amounts of *n*-alkanes in their leaf waxes. For instance, angiosperm
146 species generate significantly higher concentrations of *n*-alkanes than gymnosperms
147 (Diefendorf et al., 2011). Therefore, different plants can make quantitatively different
148 contributions to the *n*-alkane pool in soils and sediments. However, again, little effort has

been devoted to such studies on aquatic plants (emergent, floating and submerged) (e.g., Liu and Liu, 2019).

The limited attention paid to *n*-alkane distribution and isotopic data of aquatic plants (Mead et al., 2005) also leads to major uncertainties in interpreting sedimentary mid-chain vs. long-chain waxes as derived from aquatic vs. terrestrial plants. While one study has focused on plants for a subtropical wetland system (Mead et al., 2005), most research constraining *n*-alkane distributions and stable isotope compositions of aquatic plants have been based on middle to high latitude or altitude sites (e.g., Aichner et al., 2010a, b, 2017; Duan et al., 2014). Various studies have focused on plant-derived *n*-alkanes and one or the other of their δ^2H or $\delta^{13}C$ values, but fewer studies examined *n*-alkane δ^2H and $\delta^{13}C$ values at the same time (Pedentchouk et al., 2008; Seki et al., 2010; Feakins et al., 2018; Freimuth et al., 2019). However, to the best of our knowledge no study has attempted to systematically characterize *n*-alkane distributions, abundances and isotopic signals (δ^2H and $\delta^{13}C$) for both leaves and roots of wetland plants. Such data are needed to decrease uncertainty in interpreting sedimentary *n*-alkane signals in aquatic ecosystems, such as differentiating source vegetation (Cooper et al., 2015), detecting vegetation shifts, and paleoclimate reconstruction (Sachse et al., 2012).

Investigating the dominant plant species from different ecosystems within the Everglades is an important aspect for potential paleo-reconstruction of this wetland. Our previous studies have examined leaf wax *n*-alkanes and $\delta^{13}C$ values for a variety of terrestrial and aquatic plants in the Everglades (Mead et al., 2005). More recently, leaf wax *n*-alkanes δ^2H and $\delta^{13}C$ values of 4 aquatic plant species (He et al., 2016a) was reported, and *n*-alkane δ^2H values of 3 mangrove species growing in Shark River Estuary of the Everglades were also investigated (He et al., 2015b, 2017). In this context, the present study was designed to expand the available dataset to a more extensive number of local dominant plants, with a focus on the aquatic plants. The aims are to explore the relationships among common indicators of molecular composition including the aquatic proxy (P*aq*), average leaf wax *n*-alkanes chain length (ACL), carbon preference index (CPI), and *n*-alkane δ^2H and $\delta^{13}C$ values in the leaves and roots of a wide variety of plant species across the Everglades. In particular leaves from 30 species (24 families) and roots of six species (three families) were collected along a spatial gradient from north to south

of the Everglades, but within a relatively small geographical area (within 150 km). The specific objectives of this study were to (i) determine the variability in plant *n*-alkane distributions, abundances and the corresponding CWA δ^2H and $\delta^{13}C$ values within a spatially constrained subtropical region with similar climatic conditions, (ii) examine the difference in *n*-alkane distributions, abundances and the corresponding CWA δ^2H and $\delta^{13}C$ values between leaf and root in wetland aquatic plant species, and (iii) compare *n*-alkane δ^2H and $\delta^{13}C$ values among terrestrial and aquatic plants and assess the suitability of *n*-alkane isotopes as paleo-proxies in ecosystems with mixed inputs from both terrestrial and aquatic plants.

2. Samples and Methods

2.1. Site description and samples

Vegetation samples were collected at diverse sites across the greater Everglades freshwater marshes, the Shark River estuary, and Florida Bay (25°70′ to 24°70′N; 81°15′ to 80°30′E; less than 10 m above sea level; Fig. 1a). Since sampling locations fall within a relatively small latitudinal range and negligible altitude differences, the climatic conditions in the study region are constrained as coastal subtropical. The entire geographical scale under study here, represented less than a 1º latitude difference, with no significant variations in climatic conditions, but distinctive changes in environmental settings, including terrestrial environments, freshwater wetlands, and estuarine and oceanic environments (Fig. 1b, c, d). Numerous hydrological parameters are detailed in Table S1. All plants were grouped on the basis of the growth habitat and phylogenetic domain (Table 1). Mean annual air temperature for all locations is ~25 °C, with the difference between the warmest month (July) and the coldest month (January) less than 10 °C (Ross et al., 2000). The most significant seasonal contrast is defined by precipitation. Mean annual precipitation is ~120 cm with 21 cm falling during the dry season (December to April) and 99 cm falling during the wet season (May to November). The average relative humidity ranged from 67% to 85%, with annual average close to 75% (Price et al., 2006; Jimenez et al., 2012).

The freshwater marsh topography of the Everglades consists primarily of seasonally inundated ridge and slough landscapes with some small stands of trees on

211 higher elevations (tree islands; Fig. 1b, c, d). This wetland ecosystem is commonly
212 referred to as the "River of Grass" (Douglas, 1947), which is characterized by grassy
213 marshes dominated by sawgrass (*Cladium jamaicense*) in the emerged ridges and by
214 spikerush, bladderwort and water lily (*Eleocharis* sp.*, Utricularia* sp. and *Nymphaeaceae*
215 sp., respectively) in adjacent, more deeply submerged (lower elevation) slough
216 environments. In sharp contrast, mangrove forests are distributed along the Shark River
217 estuary and coastal fringe region and include red mangroves (*Rhizophora mangle*), black
218 mangroves (*Avicennia germinans*), and white mangroves (*Laguncularia racemosa*).
219 Seagrasses including *Thalassia testudinum, Halodule wrightii*, and *Halophila decipiens*
220 are commonly found in Florida Bay.
221 Leaves from 30 plant species (representing 24 families, 122 individual samples),
222 including terrestrial trees, shrubs and ferns, freshwater wetland plants (WCA3, Shark
223 River Slough (SRS) 1-3, Taylor Slough (TSPh) 2), mangroves (SRS4-6), and seagrasses
224 (Florida Bay), were collected from multiple field trips in 2004, 2011, and 2013 (Table 1,
225 Fig. 1a, Table S1). Roots from 6 dominant plant species (three families) of freshwater
226 wetlands (WCA3, SRS1-3, and TSPh2) were sampled in both March and May (Table 1,
227 Fig. 1, Table S2). The inundation periods varied among the freshwater wetland sites
228 (Table S1). The surface water types ranged from pure freshwater (GL tree island, WCA3,
229 SRS1-3, TSPh2) to mesohaline water (SRS4-6) and then to pure marine water (Florida
230 Bay), with surface water salinity spanning ~0 to 35 PSU. Ground water discharge is
231 important to the estuarine sites (SRS4-6) but has a very weak contribution to the GL tree
232 island site and all freshwater wetland sites (WCA3, SRS1-3 and TSPh2; Price et al.,
233 2006). In order to assess differences in the *n*-alkane distributions between above and
234 below ground biomass, roots from *T. domingensis*, *T. latifolia*, *C. jamaicense*, *E.*
235 *cellulosa*, and *Nymphaeaceae* sp. were analyzed from the freshwater wetland sites and
236 compared to the corresponding above ground biomass (Table S2).
237 All collected plants were placed in clean Ziploc bags, and stored in a cooler with
238 ice immediately after collection. After transport to the laboratory (within 8 hours max),
239 they were repeatedly (three times) rinsed with deionized water to remove dust particles,
240 frozen, freeze-dried, crushed to a fine powder and kept frozen (-20 ˚C) until analysis.
241

2.2. Extraction and semi-quantification of *n*-alkanes

Aliphatic hydrocarbons, including the *n*-alkanes, were extracted following a previously published protocol (He et al., 2015a). Briefly, freeze-dried biomass (~2 g) was subjected to sonication extraction three times (0.5 hours each) with pure dichloromethane (Optima, Fisher, USA) as the solvent. Total extracts were concentrated by rotary evaporation. The extracts were further fractionated as previously described (Jaffé et al., 2001; He et al., 2018a) by adsorption chromatography over silica gel and the aliphatic hydrocarbon fraction was obtained after elution with *n*-hexane. A known amount of squalane was then added as an internal standard to the isolated fraction. Gas Chromatography – Mass Spectrometry (GC-MS) analyses were performed on a Hewlett-Packard 6890 GC linked to a HP 5973 MS system in the electron impact (EI) ionization mode at 70 eV, and fitted with Rtx-1 column (30 m, 0.25 mm ID, 0.25 μm film thickness, RESTEK, USA). The GC oven temperature was programmed from 60 to 300 °C at a rate of 6°C/min after 1 min at the initial temperature, and was kept at 300°C for 20 min. Identification of the *n*-alkanes was performed by comparing chromatographic retention times, reported mass spectra and the mass spectral library (NIST 2008). Quantification was performed using the internal standard squalane, assuming similar response factors. We acknowledge that varying recoveries should exist for different samples, which may introduce additional uncertainty of the absolute concentration of each *n*-alkane. However, the standard deviations of most hydrocarbon concentrations were within 15% based on our procedure (He et al., 2014, 2018b). In addition, we analyzed two typical samples with known large differences in *n*-alkane distributions (*C. jamaicense* and *U. foliosa*) by both GC-FID (Flame Ionization Detector) and GC-MS. A series of *n*-alkane molecular parameters was calculated (see section 2.3), and no significant difference in these qualitative parameters was observed (Table S3). The relative standard deviations for each of the qualitative parameters were also listed in Table S3. Therefore, although our concentration of *n*-alkanes is not recovery-corrected and regarded as semi-quantitative, the relative distributions of different homologues of *n*-alkanes are meaningful.

2.3. *n*-Alkane molecular parameters

The concentration of each *n*-alkane was summed together to get the total *n*-alkane concentrations. Average *n*-alkane chain lengths (ACL; Eglinton and Hamilton, 1967), the relative abundance of mid-chain to long-chain *n*-alkanes (P*aq*; Ficken et al., 2000), and carbon preference index (CPI; Bray and Evans, 1961) were determined for all samples as shown below:

$$ACL_{23\text{-}33} = \frac{23(nC23)+25(nC25)+\cdots 31(nC31)+33(nC33)}{nC23+nC25+\cdots+nC31+nC33} \quad (1)$$

$$Paq = (n\text{-}C_{23} + n\text{-}C_{25}) / (n\text{-}C_{23} + n\text{-}C_{25} + n\text{-}C_{29} + n\text{-}C_{31}) \quad (2)$$

$$CPI_{23\text{-}33} = \frac{1}{2}\left[\frac{nC23+nC25+\cdots+C33}{nC24+nC26+\cdots C32} + \frac{nC23+nC25+\cdots+C33}{nC26+nC28+\cdots C34}\right] \quad (3)$$

2.4. Compound-specific carbon and hydrogen isotope analysis

Compound-specific $\delta^{13}C$ values of individual *n*-alkanes were measured by gas chromatography-isotope ratio mass spectrometry (GC-IRMS), using an HP 6890 GC equipped with a DB-1 fused silica capillary column (30 m, 0.25 mm ID, 0.25 μm film thickness), a combustion interface (Finnigan GC combustion IV), and a Finnigan MAT delta Plus V mass spectrometer. Between every four samples, three external standard mixtures containing *n*-heptadecane and squalane at different concentrations (30 ng/μL, 200 ng/μL and 500 ng/μL), with known $\delta^{13}C$ values of -21.3‰ and -29.5‰ (provided by Dr. A. Schimmelmann, Indiana University, Bloomington), respectively, were measured to check instrument performance during the entire analysis period and for correction purposes. The accuracy is 0.2‰ and 0.1‰ for *n*-heptadecane and squalane, respectively. For the $\delta^{13}C$ measurement, only *n*-alkanes with amplitudes higher than 1000 mVs were considered acceptable. $\delta^{13}C$ values are given in per mil (‰) notation relative to the Vienna Peedee Belemnite (VPDB) standard. Samples were analyzed at least two times, and the averaged values were reported, with standard deviation all smaller than 0.4‰ (when triplicates were available). Precision for *n*-alkane carbon isotope determinations was ±0.3‰ as determined by a co-injected secondary standard (squalane, -29.5‰).

Compound-specific $\delta^{2}H$ values of individual *n*-alkanes were measured using a GC/Pyrolysis/IRMS system consisting of a HP 6890 GC connected to a Finnigan MAT

delta Plus V mass spectrometer. The GC column and oven program described above was used. The pyrolysis temperature was set at 1440 ˚C in a micro volume ceramic tube. Helium was used as carrier gas at 1.6 mL/min. Calibrated methyl palmitate (-255‰) and squalane (-107‰) mixtures with different concentrations (200, 800 and 1200 ng/μL for each) were used as external standards. External standard calibration was performed after every four sample measurements. The F8 standard (purchased from Indiana University, Bloomington, USA) was analyzed at least every 6 samples, and had a measured accuracy of ±3‰. The H_3^+ factor was measured daily prior to sample analysis and averaged 5.0 ± 0.1 during this study. δ^2H values for each sample were normalized to the VSMOW (Vienna Standard Mean Ocean Water) scale by the nearest two F8 standards, and the internal co-injected squalane for each sample if necessary. For the δ^2H measurements, only *n*-alkanes with amplitudes higher than 1000 mVs were considered acceptable. Samples were analyzed at least two times, and the averaged values were reported, with standard deviation all smaller than 4‰ (when triplicates were available). The precision was assessed by the secondary reference material: the methyl palmitate and squalane mixed standards, and the standard deviations were 4‰ and 3‰ (n = 43) for methyl palmitate and squalane, respectively, throughout the whole analysis.

2.5. Estimations of the atmospheric $\delta^{13}C$, fresh, mesohaline and marine surface water δ^2H values

The $\delta^{13}C$ value of atmospheric CO_2 was estimated as -8.45‰, based on monthly average values during the year 2012 from Key Biscayne, Florida, United States; (http://www.esrl.noaa.gov/gmd/dv/data/). The δ^2H composition of precipitation is variable in South Florida. It is known that the precipitation δ^2H values measured at the Redlands agricultural area of South Florida (within ~80 km from all our sampling sites; Fig. 1) vary throughout the year from -50.6‰ to 2.4‰ during the wet season, and from -34‰ to 9.1‰ during the dry season (Price et al., 2008). The weighted average δ^2H value (n = 43) of precipitation at the Redlands location is -12.3‰ (Price et al., 2008), which is used as the surface freshwater δ^2H values for the freshwater wetland of the Everglades. This freshwater δ^2H value is also similar to the estimated value (~ -12 to -11‰) of mean

annual precipitation among our studying sites generated by the Online Isotopes in Precipitation Calculator (OIPC; www.waterisotopes.org; Bowen, 2019; Bowen and Revenaugh, 2003). The δ^2H values of monthly mean precipitation ranged from -12 to 4‰ generated by the OIPC. In particular, the mean δ^2H values of precipitation in March, May and August (our sampling months) ranged from -10 to -9‰, -9 to -8‰, and 4‰, respectively, from OIPC. Surface seawater in the Gulf of Mexico has an average δ^2H value of 15‰ (Sternberg and Swart, 1987). The δ^2H values of surface freshwater (-12.3‰) and marine water (15‰) are consistent with previous studies in the South Florida region, where freshwater and marine surface water values were reported to range between -14 to 15‰ (Sternberg and Swart, 1987; Price et al., 2008; Saha et al., 2009). Although leaf wax formation is limited to the brief period of spring leaf emergence in deciduous plants (e.g., Newberry et al., 2015; Freimuth et al., 2017), it may last for longer time scales (weeks to months, Jetter et al., 2006) in most of wetland plants surveyed in this study since the Everglades freshwater marsh ecosystems are recognized as oligotrophic, subtropical wetlands with a year-round growing season (Malone et al., 2013). In contrast, precipitation water δ^2H values fluctuate on short time scales (days or even hours) in coastal ecosystems such as the Everglades (Price et al., 2008). Therefore, we consider it is appropriate to use averaged annual precipitation δ^2H values rather than a single snapshot of precipitation δ^2H value at the time when the leaves were collected. Moreover, using averaged annual precipitation δ^2H values makes our data better incorporated in most of the current global calibration studies (e.g., Sachse et al., 2012; Liu and An, 2019; McFarlin et al., 2019).

2.6. Bulk $\delta^{13}C$ measurements

The $\delta^{13}C$ values of ground plant leaves and roots were obtained using a FLASH2000 Organic Elemental Analyzer coupled to a Finnigan MAT delta Plus V mass spectrometer. Samples were measured in duplicates and mean values are reported. A reference standard material (glycine) was analyzed every five measurements. The standard deviation of the replicate measurements was ±0.2‰.

The carbon isotopic fractionation factor between the atmosphere and plant leaf or root is calculated using the following equation:

$$\varepsilon_{atm\text{-}leaf\ or\ root} = ((\delta^{13}C_{atm} + 1000)/(\delta^{13}C_{leaf\ or\ root} + 1000) - 1) \times 10^3.$$

2.7. Statistics

Statistical analyses were performed using SPSS 13.0 for Windows. The unpaired Student's t-test (two-tailed) was used to compare different groups of means at $p = 0.05$ and $p = 0.01$ significance levels (unless otherwise indicated). The principal component analysis (PCA) was conducted using R3.2.1.

3. Results

3.1. *n*-Alkane abundances and distribution patterns in leaves

Vegetation was classified for discussion purposes mainly based on the classical growth habitat, and also on the phylogenetic domain (or functional types; Table 1; Fig. 2), consistent with previous studies (e.g., Diefendorf et al., 2010, 2011). *n*-Alkane abundances represented a large (two orders of magnitude) range from 2 μg/gdw in *Halophila decipiens* to 884 μg/gdw in *C. jamaicense* (Table 2; Fig. 2). The concentrations of *n*-alkanes in the two gymnosperms (*Taxodium distichum* and *Pinus elliottii*) were less than 10% of that in most of the angiosperms studied here. Similarly, low *n*-alkane concentrations (usually < 20 μg/gdw) in gymnosperms have previously been reported by Diefendorf et al. (2011). A significant positive correlation ($p<0.01$) was observed between C_{29} *n*-alkane concentration and total *n*-alkane concentrations (Fig. S1).

The distribution of *n*-alkanes in most of the plants ranged from C_{23} to C_{33} with a characteristic odd/even predominance (mean $CPI_{23\text{-}33} = 15.5 \pm 16.1$). C_{23} or C_{25} *n*-alkane was the most dominant homologue in the aquatic submerged plants (*Utricularia* sp.) and marine seagrasses (*Syringodium filiforme*, *Halodule wrightii*, *Ruppia maritima* L., and *Halophila decipiens*). The emergent aquatic plants (*Eleocharis* sp. and *Typha* sp.) were dominated by C_{25}, C_{27} or C_{29} *n*-alkane, whereas in the woody terrestrial vegetation, as well as the mangroves, the most abundant *n*-alkane was C_{29}, C_{31} or C_{33}. Within *C.*

jamaicense (the most dominant plant in the Everglades), leaf P*aq* ACL_{23-33} and CPI_{23-33} showed no significant difference between March and May (Fig. S2).

P*aq* and ACL values ranged from 0.00 to 1.00 and from 24.0 to 30.7, respectively, across the above ground vegetation samples analyzed in this study. These values are similar to those reported previously in Everglades' vegetation (Mead et al., 2005; Saunders et al., 2006, 2015; Regier et al., 2018). In general, P*aq* increased, and ACL decreased from terrestrial island (TI) plants and estuarine mangroves (MA) to freshwater wetland emergent plants (EW), freshwater wetland submerged or floating plants (SW) and marine seagrasses (MS; Fig. 3).

3.2. Comparison of abundance and distribution of *n*-alkanes in roots and leaves of freshwater wetland plants

n-Alkane abundances represented a large range (two orders of magnitude) from 2 μg/gdw in *T. domingensis* roots to 250 μg/gdw in *E. cellulosa* root in freshwater wetland plants (Table S2). *T. domingensis* leaves had significantly higher ($p< 0.05$) average *n*-alkane concentrations than their root counterparts (Table 3; Fig. 4). However, no significant difference in *n*-alkane concentrations was observed between leaves and roots for *T. latifolia* and *Nymphaeaceae* sp.. *E. cellulosa* roots had higher *n*-alkane concentrations than the leaves, although this result was not statistically significant (Table 3; Fig. 4). Similar results were observed for *M. trifoliate* and *C. dimorpholepis* in a temperate peatland, where the roots of both species had higher *n*-alkane concentrations than their leaves (Huang et al., 2011). Even when focused on long-chain *n*-alkanes (e.g., C_{29} *n*-alkane), the average concentrations of C_{29} *n*-alkane in roots were not significantly different from the leaves for *E. cellulosa*, *T. latifolia*, and *Nymphaeaceae* sp. (Fig. S3). Similarly, no significant difference between leaves and roots was observed for C_{31} and C_{33} *n*-alkanes (Fig. S3). For the mid-chain *n*-alkanes (e.g., C_{23} *n*-alkane), no significant difference between roots and leaves could be determined for all plants surveyed (Fig. S3).

Among all wetland plant roots surveyed, P*aq* and ACL values ranged from 0.32 to 0.96 and 23.7 to 27.5, respectively (Table 3). All freshwater wetland plant roots had significantly higher ($p< 0.05$) P*aq* values but lower ACL ($p< 0.05$) than their leaf counterparts (Fig. 4), in agreement with Regier et al. (2018).

3.3. Compound-specific hydrogen isotopic compositions in leaves

Since C_{29} *n*-alkane is the most common homologue used in both modern calibration and paleo-reconstruction, its δ^2H values obtained from this study were firstly compared to the latest global calibrations of the relationship between plant leaf C_{29} *n*-alkane δ^2H and mean annual precipitation δ^2H values (Sachse et al., 2012; Liu and An, 2019; McFarlin et al., 2019) (Fig. S4). All these C_{29} *n*-alkane δ^2H values fit well into the latest global calibration. Nevertheless, since the molecular distribution of *n*-alkanes was highly variable among plant growth habitats (Table S2), using the isotopic value of a single chain length *n*-alkane (e.g., C_{29} *n*-alkane) for comparison among plant species is not adequate because the same compounds are not available or present in high abundance across all species for analyses. Thus, consistent with previous comparisons across a wide range of plant species (Chikaraishi and Naraoka, 2003; Kahmen et al., 2013; He et al., 2017) CWA $\delta^{13}C$ and δ^2H values for odd carbon number *n*-alkanes from *n*-C_{23} to *n*-C_{33} were calculated (Table 2; Table S2).

The CWA *n*-alkane δ^2H values ranged from -268‰ to -78‰ among all studied plant leaves (Table 2; Table S1). In general, CWA δ^2H values differed significantly among plant living habitats (Fig. 3). Terrestrial plant (trees, shrubs and ferns) leaves had *n*-alkanes with significantly ($p < 0.05$) higher average δ^2H values (-88‰ ± 5‰, 11 species, 18 individual samples) than the adjacent wetland emergent, floating and submerged plant leaves (-148‰ ± 48‰; 8 species; 51 individual samples; Fig. 3).

The CWA *n*-alkane δ^2H values of terrestrial woody plants from the tree island ranged from -95‰ (*T. distichum*) to -78‰ (*P. borbonia*) (Table 2; Fig. 2), although they were growing at the same site. The ferns (*B. chilense* and *O. regalis*) living in the same area have intermediate CWA *n*-alkane δ^2H values of -89 ± 4‰ and -86 ± 3‰, respectively, and were similar to those of the woody plants. In contrast, the CWA *n*-alkane δ^2H values of the Everglades freshwater wetland plant leaves spanned -137‰ to -119‰ (Table 2; Fig. 2), except for leaf *n*-alkane from *C. jamaicense* which had significantly depleted CWA *n*-alkane δ^2H values (-231‰ ± 24‰, n = 10) compared to all other plants. The CWA δ^2H values of mangrove leaves (*R. mangle*, *L. racemosa*, and *A. germinans*) range from -183‰ to -122‰ (He et al., 2017), which are lower ($p < 0.05$)

than the terrestrial tree leaves from the tree island (Table 2; Fig. 2). The CWA *n*-alkane δ^2H values of the C_4-type seagrasses (*S. filiforme*, *R. maritima*, and *H. wrightii*) were -86 ± 4‰, -84 ± 5‰, and -92 ± 3‰, respectively, which were higher ($p < 0.01$) than those of the freshwater aquatic plants (averaged as -139 ± 36‰, n = 8) but similar to the C_3 tree leaves (averaged as -87 ± 6‰, n = 9; Table 2; Fig. 2).

3.4. Compound-specific and bulk carbon isotopic compositions in leaves

The C_3 plant leaf bulk $\delta^{13}C$ values ranged from -31.6‰ to -25.2‰ (Table S2), in agreement with previous studies (e.g., Mead et al., 2005). This range of leaf bulk $\delta^{13}C$ values resulted in the $\varepsilon_{atm\text{-}leaf}$ values from 16.8‰ to 23.0‰, which fit well within the regression between $\varepsilon_{atm\text{-}leaf}$ and mean annual precipitation presented by Diefendorf and Freimuth (2017), considering the annual precipitation of the Everglades is ~1200 mm/yr. The CWA *n*-alkane $\delta^{13}C$ values ranged from -41.5‰ to -25.6‰ and from -17.3‰ to -14.4‰ among studied C_3 and C_4-type seagrass plant leaves, respectively (Table 2). Similar to the δ^2H measurements, the $\delta^{13}C$ values are not reported for a few plant *n*-alkanes because of their low concentrations.

Seagrasses had significantly higher ($p < 0.01$) CWA *n*-alkane $\delta^{13}C$ values (-17.3‰ to -12.2‰) than all other C_3 plants (-41.5‰ to -25.6‰). Among all C_3 plants in the freshwater wetland and tree islands, *U. foliosa* had the lowest CWA *n*-alkane $\delta^{13}C$ values at -38.7‰ (n = 8; SD = 1.1‰). The CWA *n*-alkane $\delta^{13}C$ value from *T. distichum* was -25.6‰, which is the highest among all C_3 plants and a little lower than the corresponding bulk leaf $\delta^{13}C$ value (-22.0‰, Anderson et al., 2005). A significant negative correlation between ACL and the CWA *n*-alkane $\delta^{13}C$ values and significant positive correlation between P*aq* and the CWA *n*-alkane $\delta^{13}C$ values were observed across the whole dataset. This is mainly caused by the extremely low ACL, high P*aq* and ^{13}C-enriched signals and for marine seagrass.

3.5. Comparison of bulk carbon and compound-specific hydrogen and carbon isotopic values in roots and leaves of freshwater wetlands

The bulk $\delta^{13}C$ values of roots ranged from -28.7‰ to -22.8‰ (Table S2) in roots of freshwater wetland plants (*C. jamaicense*, *T. latifolia*, *T. domingensis*, *E. celluosa*, and

Nymphaeaceae sp.). The CWA $\delta^{13}C$ and $\delta^{2}H$ values of roots ranged from -34.1‰ to -30.6‰ and from -206‰ to -129‰, respectively (Table 3). Most of freshwater wetland plant roots had higher bulk $\delta^{13}C$ values than their leaf counterparts (Fig. 4; Fig. S5), in agreement with bulk $\delta^{13}C$ data published by Hobbie and Werner (2004). No significant differences in CWA $\delta^{2}H$ values between leaves and roots were observed for *T. latifolia* and *T. domingensis* (Fig. 4). Significantly higher $\delta^{2}H$ values were found in leaves of *E. celluosa* and *Nymphaeaceae* sp., whereas the opposite trend was observed in *C. jamaicense* ($p < 0.05$; Fig. 4). All wetland plant roots had higher CWA $\delta^{13}C$ values than their leaf counterparts. A significant difference in CWA *n*-alkane $\delta^{13}C$ values between roots and leaves was only observed in *Nymphaeaceae* sp. ($p < 0.05$; Fig. 4). The lack of significant differences in CWA *n*-alkane $\delta^{13}C$ values between roots and leaves for other plants may be due to the limited sample size.

We only obtained reliable measurements for $\delta^{13}C$ or $\delta^{2}H$ values of C_{25} *n*-alkane (a mid-chain homologue) and C_{29} *n*-alkane (a long-chain homologue) across all freshwater wetland plants (both leaves and roots). Significantly higher C_{25} *n*-alkane $\delta^{13}C$ values were found in roots of *T. latifolia* and *Nymphaeaceae* sp., and significantly higher C_{29} *n*-alkane $\delta^{13}C$ values in root of *Nymphaeaceae* sp., than their leaf counterparts (Fig. S6). Significantly higher C_{25} and C_{29} *n*-alkane $\delta^{2}H$ values were found in roots of *C. jamaicense* than its leaf counterpart, whereas the opposite trend was observed for the C_{25} *n*-alkane of *E. cellulosa* and *Nymphaeaceae* sp. (Fig. S6).

Considering our plant survey in GL tree island and freshwater wetlands was carried out in March and May, the potential seasonal variations were tested using *C. jamaicense* due to its larger sample size relative to all other plant species. Therefore, we grouped our measured parameters for *C. jamaicense* by sampling month (March vs. May, Fig. S2). The highest average total *n*-alkane concentration was observed in leaves sampled in May. The highest average P*aq* value was observed in roots sampled in March. The C_{29} *n*-alkane $\delta^{2}H$ values in roots were higher than leaves ($p < 0.05$). Average leaf C_{29} *n*-alkane $\delta^{2}H$ values were higher in March than in May, although this difference was not significant.

4. Discussion

514 Before discussing the variations in abundance and distribution of *n*-alkanes and their
515 isotopic values, we need to make two points clear, including: (i) grouping criteria of
516 Everglades wetland plants; (ii) magnitude of seasonal variations.
517 First, we grouped our plants mainly by growth habitats (including tree island plants,
518 emergent wetland pants, submerged wetland plants, estuarine mangroves and marine
519 seagrasses) instead of life form classes such as (i) trees/shrubs, forbs, and algae (Fig. S7),
520 or (ii) fern, gymnosperms, monocots, dicots, and algae (Fig. S8), which have been
521 applied in other studies focusing mainly on terrestrial ecosystems (e.g., Sachse et al.,
522 2012; Diefendorf and Freimuth, 2017). The latter two groupings by life form have more
523 limitations than that of growth habitat. For instance, the forbs grouping in Fig. S7 spans a
524 wide range of $\delta^{13}C$ values since it also contains a few marine seagrass species, while (ii)
525 the monocots include both freshwater wetland plants (^{13}C depleted, <-30‰) and marine
526 seagrass (*S. filiforme* and *R. maritima* L.) with a very enriched ^{13}C signal (>-20‰; Fig.
527 S8). Because seagrasses are adapted to such a different habitat than those occupied by
528 terrestrial forbs or monocots, grouping plants primarily by growth habitat is most logical
529 for comparing the impact of changing vegetation sources on the distribution and isotopic
530 composition of *n*-alkanes in the sediments of a wetland ecosystem such as the Everglades.

531 Secondly, our samples were obtained from three months (March, May and August),
532 but wax synthesis mostly occurs during the growing season (e.g., Sachse et al., 2010;
533 Tipple et al., 2013; Freimuth et al., 2017). Monthly variations in wax synthesis might
534 introduce variations in our measured proxies. Although the wet season (May to
535 November) is the primary growing season for most of plant species (Ewe and Sternberg,
536 2003; Newman et al., 1996), the freshwater marsh ecosystems of the Everglades are
537 oligotrophic, subtropical wetlands with a year-round growing season (Malone et al.,
538 2013). Leaf wax *n*-alkane δ^2H values could mainly reflect leaf water δ^2H values at the
539 time of leaf formation (Sachse et al., 2010; Tipple et al., 2013; Freimuth et al., 2017), or
540 the leaf wax *n*-alkane δ^2H values could vary temporally, which has been observed in four
541 riparian plant species (Oakes and Hren, 2016; Huang et al., 2018). Similar variations
542 were observed for *C. jamaicense* (Fig. S2e; Table S1). The leaf C_{29} *n*-alkane δ^2H value
543 obtained in March was higher than May leaf in the most dominant (>60% by coverage;

544 Table 1) freshwater wetland species, *C. jamaicense* (Fig. S2e). We expected that as
545 leaves reached full expansion and *n*-alkane production intensified (from early March to
546 May), simultaneous ^{2}H depletion in C_{29} *n*-alkane $\delta^{2}H$ was observed, likely caused by (i)
547 sufficient cuticular development to prevent increased leaf water ^{2}H-enrichment from
548 transpiration, (ii) metabolic shifts from heterotrophic status to autotrophic status, leading
549 to more incorporation of ^{2}H-depleted NADPH from photosystem I (Freimuth et al., 2017).
550 However, more field sampling and greenhouse studies are necessary to further justify this
551 interpretation. Due to the limitation of our sampling strategy, it is difficult to assess how
552 seasonal variation (if any) would contribute to the *n*-alkane $\delta^{2}H$ variations among our
553 dataset and the dominant underlying mechanisms. Nevertheless, our initial design is to
554 capture the *n*-alkane isotopic signal across diverse habitats (tree island, freshwater
555 wetland, estuary and marine environment). In addition, the monthly variation in *n*-alkane
556 distribution proxies and isotopic compositions observed in leaves of *C. jamaicense* are
557 not significant (Fig. S2b-f), leading us to speculate that seasonal variation (March vs.
558 May in this study) is likely not the dominant factor affecting *n*-alkane distribution for
559 Everglades wetland plants.

560 With the two points specified above, we think it should be appropriate to compare
561 both *n*-alkane distribution and isotopic proxies among Everglades plants from tree islands,
562 freshwater wetlands, the mangrove estuary, and Florida Bay.
563

564 **4.1. Variations in distribution of *n*-alkanes and their $\delta^{2}H$ and $\delta^{13}C$ values in**
565 **Everglades plant leaves**

566 ACL and P*aq* are two widely used qualitative parameters to differentiate leaf *n*-
567 alkanes derived from different plants and plants living under different climates or habitats
568 (e.g., Ficken et al., 2000; Bush and McInerney, 2013). ACL has been found to be lower
569 in plants from cooler climates compared to those from warmer climates at regional scales
570 (Simoneit, 1977; Bush and McInerney, 2013), but temperature does not appear to be a
571 strong control on ACL at a global scale (Diefendorf and Freimuth, 2017). Recent studies
572 of extant plants suggest that both biology and climate may influence ACL values (e.g.,
573 Freeman and Pancost, 2014). P*aq* is by far one of the most useful proxies differentiating

plants by its living habitats across the Everglades (Fig. 2), and within the freshwater wetland of the Everglades (Saunders et al., 2015; He et al., 2016a). The different ACL and P*aq* values and their broad ranges across different plant growth habitats (Fig. 3) within the same climate suggests that they are mainly indicative of community composition in the Everglades, rather than temperature or moisture availability. These ratios of *n*-alkane distributions could provide useful paleo-ecological information in aquatic ecosystems with both terrestrial and aquatic plant inputs, consistent with the previous review by Diefendorf and Freimuth (2017).

The range of CWA *n*-alkane δ^2H values in this study generally agreed with those reported in previous studies of modern plants from other locations world-wide, such as Japan, Europe, Thailand, the USA, and China (Chikaraishi and Noraoka, 2003; Liu et al., 2006; Sachse et al., 2006; Hou et al., 2007; Gao et al., 2014). Higher CWA *n*-alkane δ^2H values were observed in terrestrial trees than those of freshwater aquatic plants (Fig. 3), in agreement with previous studies (Chikaraishi and Naraoka, 2003; Sachse et al., 2004). Several factors can lead to the observed variability in CWA δ^2H values between terrestrial trees and freshwater wetland aquatic plants. Within freshwater wetland aquatic plants, a wide range of CWA *n*-alkane δ^2H values were observed. *C. jamaicense* had the lowest CWA *n*-alkane δ^2H value (Table 2, Table S2), which could be caused by factors including (i) biosynthetic mechanisms specific to sawgrass, resulting in a stronger isotopic depletion compared with other wetland plants, (ii) differences in the timing of lipid biosynthesis, or (iii) differences in source water δ^2H values or different leaf water enrichment (Goslee and Richardson, 2008). Metabolic differences are often hypothesized to explain differences in biosynthetic fractionation among plant groupings (e.g., Cormier et al., 2018), such as between terrestrial trees and aquatic plants, or within aquatic plants. The source water δ^2H values may not be a dominant factor, considering the precipitation δ^2H values were consistent among our study sites, surface water δ^2H values were very similar within the freshwater wetland sites, and ground water input was limited in the freshwater wetland sites (Price et al., 2006, 2008; Table S1). However, whether leaf water enrichment is an important factor contributing to large variation in *n*-alkane δ^2H values (e.g., largest depletion in ^2H for *C. jamaicense*) needs further investigation, given the lack of measurements in this study. Because of the highly widespread distribution (>

605 60% by coverage) of *C. jamaicense* and its significantly lower δ^2H values, it has been
606 applied to assess the historic vegetation succession in Everglades wetlands (He et al.,
607 2016a).
608 The lower CWA *n*-alkane δ^2H values observed in mangroves, compared to those
609 of terrestrial tree island trees, were unexpected at first glance since estuarine brackish
610 water is more ^2H enriched than fresh water (Price et al., 2008; He et al., 2017). However,
611 similarly ^2H-depleted *n*-alkane δ^2H values have previously been reported for *Avicennia*
612 *marina*, *Rhizophora* sp., and *Bruguiera gymnorhiza* leaves, and have been mainly
613 attributed to (i) increased discrimination against ^2H during symplastic uptake of saline
614 water, (ii) enhanced production of compatible solutes from ^2H-enriched pyruvate, or (iii)
615 different gradients in relative humidity and/or water vapor isotopes at the leaf surface
616 (Ladd and Sachs, 2012, 2015, 2017).
617 The averaged δ^2H values of marine surface water (15‰) is ~27‰ higher than that
618 of the surface freshwater (-12.3‰) in Florida Everglades (Table S1; Price et al., 2008;
619 Saha et al., 2009; He et al., 2017), but similar CWA *n*-alkane δ^2H values were observed
620 between seagrasses and C_3 tree leaves, suggesting different biosynthetic fractionation
621 processes are likely. Although no significant difference in δ^2H values of lipids among
622 plants with different biosynthetic pathways was reported by Sternberg et al. (1984), a
623 subsequent study by Chikaraishi and Naraoka (2003) showed that δ^2H values of leaf wax
624 from C_3 plants were slightly more enriched than those of C_4 plants, and suggested that the
625 difference in δ^2H values could be associated with differences in evapotranspiration and *n*-
626 alkane biosynthetic fractionation.
627 Water availability, light intensity, temperature, humidity, latitude and atmospheric
628 $\delta^{13}C$ of CO_2 can cause variability in $\delta^{13}C$ values among C_3 plant leaves (Kohn, 2010;
629 Diefendorf et al., 2011; Diefendorf and Freimuth, 2017). However, these factors are
630 unlikely to be a significant cause of variability in our study, since all these C_3 plant leaves
631 were restricted along a relatively small spatial gradient, with very similar environmental
632 factors stated above. Rather, the variations among C_3 plants in the Everglades are more
633 likely to be influenced by plant type and its local habitat (Freeman et al., 2011). The
634 submerged freshwater vegetation *Utricularia* sp. resulted in a particularly light isotopic
635 signal (Table 2), which may be caused by the utilization of carbon dioxide derived from

636 recycled OM of terrestrial or aquatic plants, or soil/sediment (Keough et al., 1998; Mead
637 et al., 2005).

638 **4.2. Comparison of abundances and distribution of *n*-alkanes and their δ^2H and**
639 **$\delta^{13}C$ values in roots and leaves of the freshwater wetland plants**

640 No significant differences in *n*-alkane abundances are observed between leaves
641 and roots in wetland aquatic plants such as *Nymphaeaceae* sp., and the average *n*-alkane
642 concentration is even higher in the roots than leaves in the case of *E. cellulosa*. With
643 organ-specific biomass data (both leaves and roots) reported previously (Saunders et al.,
644 2006, 2015), the contribution of leaf and root *n*-alkanes to surface sediments was
645 estimated for the aquatic plant species *C. jamaicense*, *E. cellulosa*, *Nymphaeaceae* sp., *T.*
646 *latifolia*, and *T. domingensis* (Tables S4, S5), following the approach presented in
647 Gamarra and Kahmen (2015). Considering the relative proportion of leaf and root
648 biomass produced by each species, root-derived total *n*-alkane contributions to the
649 sediment record are approximately 10% of leaf contributions for all plants except *E.*
650 *cellulosa* (Table S4) and somewhat smaller when restricted to the C_{29} *n*-alkane (Table S5).
651 For *E. cellulosa*, the contribution of root-derived *n*-alkanes to sediments is higher than
652 those of leaves when estimated for total *n*-alkanes (Table S4), but only 25% of leaf
653 contributions when restricted to the C_{29} *n*-alkane (Table S5). These simple mass balance
654 calculations confirm that the dominant long-chain *n*-alkanes (e.g., C_{29} *n*-alkane) are
655 primarily derived from leaves rather roots across all Everglades freshwater wetland
656 species surveyed. However, when restricted to mid-chain *n*-alkanes such as C_{23} *n*-alkane,
657 a different story was revealed. The contribution of root-derived C_{23} *n*-alkanes to
658 sediments is 7 times higher than leaf-derived C_{23} *n*-alkane contribution in *Eleocharis* spp.
659 (Table S5). The contribution of root-derived C_{23} *n*-alkanes to sediments is 54% of leaf
660 contributions in *T. latifolia*, 40% in *T. domingensis*, 22% in *C. jamaicense*, and 13% in
661 *Nymphaea* spp., respectively (Table S5). Therefore, although root-derived *n*-alkanes may
662 not be the dominant input of long-chain *n*-alkanes, they could be a considerable input of
663 mid-chain *n*-alkanes (e.g., C_{23} *n*-alkane) in Everglades freshwater wetland sediments
664 (Table S5).

665 Although this study reports a simple proportion of *n*-alkane concentrations derived
666 from leaves and roots under modern conditions, environmental conditions such as the

667 effects of temperature and aridity could affect plant leaf and root-derived *n*-alkane
668 distributions and in turn their relative contributions to sediments (Jansen and Wiesenberg,
669 2017). Significantly higher P*aq* and lower ACL values were observed in roots than in
670 leaves, which may be a result of increased evapotranspiration pressure in leaves, as
671 cuticles with higher abundances of longer chain *n*-alkanes (*n*-C_{29} and *n*-C_{31}) may form an
672 epicuticular barrier to reduce the loss of water in leaves (e.g., Eglinton and Hamilton,
673 1967; Hauke and Schreiber, 1998). Considering the relatively high turnover rates (ca. ~55%
674 per year) of roots in wetland ecosystems (Gill and Jackson, 2000), the higher P*aq* and
675 lower ACL values of roots relative to leaves may have a significant impact on these
676 values in sediments or soils from Everglades freshwater wetlands (Saunders et al., 2015).
677 Therefore, contributions of *n*-alkanes from leaves and roots to sediments are likely to
678 vary in complex ways across and within species over time and space, suggesting the need
679 to investigate root-derived *n*-alkane abundances and distributions in other aquatic plants
680 and aquatic environments. Studies combining microfossils and multiple lipid biomarkers
681 are encouraged to provide more robust information about vegetation and hydrological
682 change from soil profiles, avoiding potential misinterpretation due simply to differential
683 inputs of root and leaf material downcore (Saunders et al., 2015).
684 Although only a few comparative studies exist so far, significant differences in *n*-
685 alkyl lipid δ^2H and $\delta^{13}C$ values between autotrophic and heterotrophic plant organs
686 (leaves vs. roots) have been observed previously (Dungait et al., 2011; Gamarra and
687 Kahmen, 2015; Liu et al., 2019). Dungait et al. (2011) suggested that a range of post-
688 photosynthetic fractionation effects may cause the difference in fatty acid $\delta^{13}C$ values
689 between flowers and leaves. Gamarra and Kahmen (2015) investigated 15 species of
690 European C_3 grasses and found *n*-alkane δ^2H values of carbon autonomous plant organs
691 (leaves and stems) were lower compared to the non-carbon autonomous organs such as
692 roots and inflorescences, which agrees with the observations of *C. jamaicense* in this
693 study. These organ-specific δ^2H values may be caused by differences in the biosynthetic
694 origin of H in NADPH used for *n*-alkane synthesis in different plant organs (Gamarra and
695 Kahmen, 2015). However, this relationship was not observed in *E. cellulosa* and
696 *Nymphaeaceae* sp., where lower CWA *n*-alkane δ^2H values were observed in the root
697 than the leaf. Similarly, such differences were also not observed in two grasses and one

shrub species sampled from the Chinese Loess Plateau (Liu et al., 2019). Considering the different environments between the subtropical freshwater wetland in this study, the alpine and temperate grasslands studied by Gamarra and Kahmen (2015), and the grasses and shrubs from the Chinese Loess Plateau (Liu et al., 2019), other factors may explain these contrasting results. In general, the observed differences in δ^2H and $\delta^{13}C$ values between leaves and roots, while limited to only a few species, indicate the existence of different biosynthetic depletion mechanisms during *n*-alkane synthesis, which would lead to some limitations for the paleo-reconstruction in aquatic ecosystems. In particular, an increasing number of studies use relative abundances and isotopic compositions of both mid-chain and long-chain *n*-alkanes for paleo-reconstruction in aquatic systems (e.g., Arnold et al., 2018; Taylor et al., 2019). Because of the high abundance of mid-chain *n*-alkanes in aquatic plant roots, and the density of root material in wetland sediments, more studies are encouraged to better constrain the impact of root-derived compounds on the integrated *n*-alkane signal in such sediments.

4.3. Implications for source differentiation in wetland ecosystems

A strong correlation has been well established between leaf wax *n*-alkane δ^2H values in modern terrestrial plants (or sediments) and precipitation δ^2H values at the global scale (Sachse et al., 2012; Liu and An, 2019; McFarlin et al., 2019). Precipitation δ^2H values exercise first order control of plant leaf wax *n*-alkane δ^2H values on a global scale. However, all the plants in this study were sampled within a small area, with no significantly different mean annual precipitation δ^2H values based on OIPC among sampling sites (see section 2.5). The variation in surface water δ^2H values among tree island (-12.3‰), freshwater wetland (-12.3‰), estuarine and oceanic environments (-12.3‰ to 15.0‰; Table S2) would only account for up to ~27‰ difference in the source water used by Everglades plants, which may lead to ~27‰ variations in the CWA *n*-alkane δ^2H values. Although groundwater discharge was important in estuarine sites (SRS4-6; Price et al., 2006), it was not significant in the GL tree island and freshwater wetlands, whereas surface water or water with similar δ^2H values to the surface water may still be the dominant source of water used by Everglades plants. With small variability among surface and precipitation water δ^2H values (up to 27‰), this study documents a large

range of CWA *n*-alkane δ^2H values within a short geographic scale, and vast differences (up to 153‰ within the freshwater wetland, and ~5 times higher than the likely variability among source water δ^2H values) among different plant growth habitats (Fig. 3; Figs. S7, S8). Therefore, the significant variation in CWA *n*-alkane δ^2H values may suggest that biosynthetic hydrogen isotope fractionations are likely different between aquatic and adjacent terrestrial plants, similar to that seen by Gao et al. (2011) in lake sediments, or between freshwater aquatic plants and marine seagrasses, terrestrial tree island plants and mangroves (Fig. 3). Similarly, although the $\delta^{13}C$ value of the atmosphere CO_2 is constant for all the plants, significant differences ($p < 0.05$) in CWA *n*-alkane $\delta^{13}C$ values were observed among wetland plant leaves, such as *T*. *domingensis* vs. *T*. *latifolia*, and between roots and leaves of the same wetland plants (Fig. 4). These large variations in both *n*-alkane δ^2H and $\delta^{13}C$ values are notable and set a foundation for source differentiation in the sedimentary *n*-alkanes, since they are derived from multiple plants and both the leaves and roots within this and similar wetland settings.

One significant limitation in using long-chain *n*-alkanes as biomarkers exclusive of terrestrial higher plants is that they can also potentially be derived from other sources such as aquatic plants (Pancost and Boot, 2004). Aquatic plants, especially freshwater emergent plants, also produce a considerable proportion of long-chain *n*-alkanes (e.g., Ficken et al., 2000; Mead et al., 2005), resulting in smaller differences in ACL and P*aq* between terrestrial and aquatic emergent plant leaves. For instance, the ACL of *E*. *cellulosa* (28.2 ± 1.87) is similar to most of the terrestrial plant leaves surveyed (28.04 to 30.73). The P*aq* of *T*. *latiforlia* leaf (0.13 ± 0.05) is similar to that of *M*. *virginiana* leaf (0.10 to 0.14), *P*. *elliottii* (0.20), *P*. *borbonia* (0.21), and *T*. *distichum* (0.17). In addition, there is no significant difference in CWA *n*-alkane $\delta^{13}C$ values between the leaf of *T*. *latifolia* and *M*. *virginiana*, suggesting that even $\delta^{13}C$ values of *n*-alkanes alone are not always useful in distinguishing between and aquatic and terrestrial plant sources (Spooner et al., 1994). However, the CWA *n*-alkane δ^2H value in the leaf of *M*. *virginiana* is significantly higher ($p < 0.05$) than that of *T*. *latifolia*, providing another dimension to differentiate *n*-alkane source between these two species. In addition to aquatic plants, algae can also contribute directly or indirectly to *n*-alkanes in sediments with varying amounts in aquatic ecosystems (Liu and Liu, 2016). For instance, Grice et al.

760 (1998) have shown that odd carbon-numbered *n*-alkanes such as C_{27} and C_{29} in sediments
761 in systems rich in *Botryococcus braunii* are derived in part from *n*-alkadienes and *n*-
762 alkatrienes generated by *B*. *braunii*, which further complicates the source assignments of
763 *n*-alkanes in sediments. Luckily, *n*-alkadienes and *n*-alkatrienes derived from *B*. *bruannii*
764 usually share significantly lower $\delta^{13}C$ values than those of *n*-alkanes (He et al., 2018a).
765 Therefore, in addition to *n*-alkane distribution, the coupling of $\delta^{2}H$-$\delta^{13}C$ two-dimensional
766 analysis is a promising tool to better discriminate between terrestrial plant-derived and
767 aquatic emergent plant derived *n*-alkanes in wetland soils and sediments.
768
769 **4.4. Implications for paleo-reconstruction in wetland ecosystems**
770 In a big picture sense of the Everglades plant isotopic data, the differences in the *n*-
771 alkane $\delta^{2}H$ composition are larger among freshwater wetland plants (e.g., submerged
772 aquatic plants vs. emergent *C*. *jamaicense*; Fig. 3, Table 1) than (i) the difference
773 between the roots and leaves of a specific species (Fig. 4), and (ii) the difference between
774 terrestrial tree island plants and submerged aquatic plants (Fig. 3, Table 1). Therefore, the
775 large variation of isotopic composition within freshwater aquatic plants present a
776 challenge for source attribution and interpretation of integrated plant-derived *n*-alkanes
777 (both terrestrial and aquatic sources) in wetland sediments.
778 In order to test if the combination of *n*-alkane distributions and the $\delta^{2}H$-$\delta^{13}C$ values
779 is useful to differentiate among plant functional type or living habitats and thus could be
780 further applied for paleo-reconstruction, we firstly compared the *n*-alkane distribution
781 and the $\delta^{2}H$-$\delta^{13}C$ values between wetland plants and surface sediments (Table S6, Fig.
782 S9). P*aq*, $ACL_{23\text{-}33}$ and C_{29} *n*-alkane $\delta^{2}H$ values all indicated that inputs from freshwater
783 wetland plants, rather than tree island vegetation, were the dominant source of wax *n*-
784 alkanes to the surface sediments. The averaged C_{29} *n*-alkane $\delta^{13}C$ value in surface
785 sediments is significantly higher than that of the tree island plants and freshwater wetland
786 plant leaves. Similar significant ^{13}C enrichments of long chain *n*-alkane from plant leaves
787 to soils was also observed in previous open plant-soil systems (Tu et al., 2004;
788 Chikaraishi and Naraoka, 2006). The reason for large $\delta^{13}C$ shifts (up to 3‰ in average for
789 C_{29} *n*-alkane) is not clear, but likely include diagenetic effects, variability in carbon
790 isotopic compositions among different plants, and external carbon inputs from soil

791 microbes and fauna (Chikaraishi and Naraoka, 2006; Wang et al., 2014). Diagenesis is
792 evidenced by significant higher CPI_{23-33} values in freshwater wetland plant leaves than
793 that of the surface sediments. A recent study by Li et al. (2018) suggests that the aerobic
794 microbes can produce considerable amounts of long-chain *n*-alkanes (e.g., C_{29} *n*-alkane)
795 in peaty soils, which complicate the application of leaf waxes in paleo-climate studies. Li
796 et al. (2018) found that microbial production rates of long-chain *n*-alkanes reached 0.1%
797 per year in aerobic conditions. Based on this production rate, modeled microbial
798 contribution of C_{29} *n*-alkanes in aerobic layers of soil, lake sediment or peatland
799 environments over timescales of 10–1000 years could approach ~1% to 35% (although
800 this range is exaggerated, given that anaerobic conditions develop as sediments are
801 buried). In the Everglades freshwater wetlands (WCA3, SRS1-3 and TSPh2),
802 microbially-derived carbon inputs are supported by other studies documenting the
803 presence of algal-derived botryococcenes (Gao et al., 2007), short-chain mono-
804 methylated alkanes (He et al., 2015b), C_{25} highly branched isoprenoids (He et al., 2016b),
805 *n*-alkadienes and *n*-alkatrienes (He et al., 2018a).
806 Secondly, we examined sediment data from cores collected in an adjacent slough
807 (basal age 160 BC) and ridge (1675 AD) at the freshwater site SRS2 (Table S6, He et al.,
808 2016a), along with the plant data from this study. A principal component analysis (PCA)
809 was performed, and 90.8% of the variability between the plant species and core
810 sediments could be explained by the first three components when combining all five of
811 the measured *n*-alkane based quantitative and qualitative fingerprints (*n*-alkane
812 concentration, ACL, P*aq*, CWA $\delta^{13}C$ and $\delta^{2}H$ values) (Fig. 5). PC1 explained 49.0% of
813 data variance, and the most positive PC1 loading was observed for P*aq*, while most
814 negative PC1 loading observed for ACL. The PC2 (22.3% of data variance) highlighted
815 $\delta^{2}H$ as a powerful discriminator among the freshwater wetland plants and mangroves
816 (^{2}H-depleted), and the marine seagrasses and terrestrial island plants (^{2}H-enriched).
817 Along the PC3 (19.6% of variance), the *n*-alkane concentration was the dominant
818 discriminator, with higher *n*-alkane concentration for *Chrysobalanus icaco* and *C.*
819 *jamaicense* helping to distinguish them from the terrestrial island and freshwater wetland
820 plants, respectively. Both the slough and ridge core samples showed intermediate PC1
821 and higher PC2 values, grouping tightly together with the freshwater wetland plants,

822 suggesting the dominant *n*-alkane input was from freshwater wetland plants instead of
823 tree island plants. In general, the different plant groups can be well differentiated by PCA
824 based on $\delta^{13}C$, $\delta^{2}H$, ACL, and P*aq*. Since vegetation is a potential major driver of *n*-
825 alkane distributions and their associated isotopic compositions, site-specific values from
826 modern samples would be important to assess historical changes in vegetation down core
827 (from the same or nearby sites). Nevertheless, the PCA approach presented here is still
828 preliminary and further studies combining plant calibration and down core measurements
829 are needed in order to test the broader applicability of the $\delta^{2}H$-$\delta^{13}C$ analysis to the
830 paleorecord in other wetland ecosystems.
831 This study presents a first comprehensive investigation of abundances, distribution,
832 $\delta^{2}H$ and $\delta^{13}C$ values of *n*-alkanes from plant species across a terrestrial-coastal-oceanic
833 gradient. We have revealed that most of metrics (*n*-alkane distribution proxy and isotopic
834 signals) differed among plant growth habitats and between leaf and root of some aquatic
835 plants. We documented that plant leaf wax was still the dominant source of long chain *n*-
836 alkanes to surface sediments, compared to roots. However, roots of some aquatic plants
837 could be an important source of mid-chain *n*-alkanes to sediments in the freshwater
838 wetlands, providing more ^{13}C enriched material and more ^{2}H enriched or depleted
839 material relative to leaves (Fig. S6). Moreover, considering the larger variation of *n*-
840 alkane isotopic signals (both $\delta^{2}H$ and $\delta^{13}C$) within freshwater aquatic plants than that
841 within the terrestrial tree island plants, PCA based on both *n*-alkane distribution proxies
842 and isotopic data could serve as a valuable tool differentiating organic matter source in
843 wetland sediments. Nevertheless, some limitations still exist, such as (i) the lack of
844 seasonal investigations of wetland plant (leaves and roots) waxes, and synchronous
845 measurements of xylem and leaf water $\delta^{2}H$ values; (ii) limited understanding of the
846 contribution of microbially derived mid- and long-chain *n*-alkanes in the aquatic
847 ecosystems; (iii) lack of mechanistic understanding of how diagenesis affects the *n*-
848 alkane isotopic signal in wetland settings; (iv) limited understanding of how both
849 vegetation shifts (i.e., emergent vs. submerged; *C. jamaisense* vs *Utricularia* sp.; if any)
850 and paleohydrology signals (i.e., precipitation and evaporation balance) contribute to
851 down-core profiles of *n*-alkane $\delta^{2}H$ values, which are critical to reconstruct historical
852 $\delta^{2}H_{water}$ or $\delta^{2}H_{precipitation}$ values. With currently available data, it is difficult to overcome all

853 of these limitations, which introduce uncertainty in deriving generalizable relationships
854 for paleo-reconstruction in wetlands. Nevertheless, the results from the current study
855 suggest that it may make more sense to target a sediment core in which no strong
856 vegetation shift seems to have occurred (e.g., small variation in P*aq*) in order to provide a
857 clearer signal for paleo-precipitation reconstruction.
858
859 **5. Conclusions**
860 The *n*-alkane abundances and distributions among leaves from different plants
861 improve our understanding of the molecular signal preserved in the Everglades
862 soils/sediments, and provides a useful context for the interpretation of δ^2H and $\delta^{13}C$
863 values from the geologic past in this and other subtropical wetland ecosystems. Although
864 our study was performed within a limited geographical scale, the abundance and
865 distribution of *n*-alkanes and their $\delta^{13}C$ and δ^2H values showed large variations among
866 plant leaves and also between above and below ground biomass components. The $\delta^{13}C$
867 values of *n*-alkanes showed large variations even within C_3 plants. *n*-Alkanes from
868 terrestrial trees and seagrasses had higher δ^2H values (by up to ~160‰) compared with
869 those of freshwater wetland macrophytes. A significant difference in *n*-alkane CWA δ^2H
870 values was observed between leaf and root counterparts of some wetland aquatic plants;
871 i.e., the CWA δ^2H value is more depleted in roots compared with its leaf counterpart for
872 the emergent plant *E. cellulosa*. *n*-Alkanes from wetland plant roots all have higher
873 averaged CWA $\delta^{13}C$ than that of leaves. Although long-chain *n*-alkanes (e.g., C_{29} *n*-
874 alkane) were shown to be predominantly derived from leaves in the freshwater wetland
875 plants, roots could contribute a considerable amount of mid-chain *n*-alkanes (e.g., C_{23} *n*-
876 alkane) to wetland sediments. These differences suggest that studies using *n*-alkanes and
877 their isotope values to track paleoclimate or paleoecology need to consider concentration
878 and composition of *n*-alkanes from both above and below ground biomass, especially in
879 ecosystems with considerable freshwater emergent plant vegetation. Although some
880 limitations still exist and necessitate further investigations, PCA combining all the
881 individual *n*-alkane proxies (abundances, distribution proxies and isotopic values) seems
882 to be a promising tool for resolving OM sources and relative contributions from key
883 Everglades plant groups. Similar studies are encouraged to further refine the use of *n*-

alkanes and their isotopic compositions for paleo-reconstruction, particularly in different aquatic settings with inputs from both terrestrial and aquatic plants, and considerable inputs from root production and turnover.

Acknowledgments

The authors appreciate the assistance of J. Harris, Dr. L. Belicka, Dr. W.T. Anderson, Dr. D. Sachse and Dr. J. Sachs during the sampling and isotope measurements. We are also grateful to Dr. X. Cui, two anonymous reviewers, and the Associated Editor: Professor Jessica Tierney for their constructive comments. D.H. acknowledges support from National Science Foundation of China [41973070; 41773098]. This work was funded by the NSF through the Florida Coastal Everglades LTER program (DEB-1237517) and contract #4600002783 by the SFWMD to RJ. R.J. and D.H. acknowledge additional support through the George Barley Endowment and the Cristina Menendez Fellowship respectively. D.H. acknowledge additional support from the hundred talent program of Zhejiang University [188020*194231701/008]. This is contribution number XXX of the Southeast Environmental Research Center at Florida International University.

References

Aichner, B., Herzschuh, U., Wilkes, H. (2010a). Influence of aquatic macrophytes on the stable carbon isotopic signatures of sedimentary organic matter in lakes on the Tibetan Plateau. Organic Geochemistry, 41(7), 706-718.

Aichner, B., Herzschuh, U., Wilkes, H., Vieth, A., Böhner, J. (2010b). δD values of *n*-alkanes in Tibetan lake sediments and aquatic macrophytes–A surface sediment study and application to a 16 ka record from Lake Koucha. Organic Geochemistry, 41(8), 779-790.

Aichner, B., Hilt, S., Périllon, C., Gillefalk, M., Sachse, D. (2017). Biosynthetic hydrogen isotopic fractionation factors during lipid synthesis in submerged aquatic macrophytes: Effect of groundwater discharge and salinity. Organic Geochemistry, 113, 10-16.

Anderson, W.T., Sternberg, L.S.L., Pinzon, M.C., Gann-Troxler, T., Childers, D.L., Duever, M. (2005). Carbon isotopic composition of cypress trees from South Florida and changing hydrologic conditions. Dendrochronologia, 23(1), 1-10.

Arnold, T.E., Diefendorf, A.F., Brenner, M., Freeman, K.H., Baczynski, A.A. (2018). Climate response of the Florida Peninsula to Heinrich events in the North Atlantic. Quaternary Science Reviews, 194, 1-11.

Bi, X., Sheng, G., Liu, X., Li, C., Fu, J. (2005). Molecular and carbon and hydrogen isotopic composition of *n*-alkanes in plant leaf waxes. Organic Geochemistry, 36(10), 1405-1417.

Bowen, G. J. (2019). The Online Isotopes in Precipitation Calculator, version 3.1. URL. http://wateriso.utah.edu/waterisotopes/pages/data_access/oipc.html.

Bowen, G. J., Revenaugh, J. (2003). Interpolating the isotopic composition of modern meteoric precipitation. Water Resources Research, 39(10).

Bray, E.E., Evans, E.D. (1961). Distribution of *n*-paraffins as a clue to recognition of source beds. Geochimica et Cosmochimica Acta, 22(1), 2-15.

Busch, J., Mendelssohn, I.A., Lorenzen, B., Brix, H., Miao, S. (2004). Growth responses of the Everglades wet prairie species *Eleocharis cellulosa* and *Rhynchospora tracyi* to water level and phosphate availability. Aquatic Botany, 78(1), 37-54.

Bush, R.T., Mcinerney, F.A. (2013). Leaf wax *n*-alkane distributions in and across modern plants: implications for paleoecology and chemotaxonomy. Geochimica et Cosmochimica Acta, 117(117), 161-179.

Cernusak, L.A., Tcherkez, G., Keitel, C., Cornwell, W.K., Santiago, L.S., Knohl, A., Barbour, M.M., Williams, D.G., Reich, P.B., Ellsworth, D., Dawson, T.E., Griffiths, H.G., Farquhar, G.D., Wright, I.J. (2009). Why are non-photosynthetic tissues generally ^{13}C enriched compared with leaves in C_3 plants? Review and synthesis of current hypotheses. Functional Plant Biology, 36(3), 199-213.

Chikaraishi, Y., Naraoka, H. (2003). Compound-specific δ^2H–$\delta^{13}C$ analyses of *n*-alkanes extracted from terrestrial and aquatic plants. Phytochemistry, 63(3), 361-371.

Chikaraishi, Y., Naraoka, H. (2006). Carbon and hydrogen isotope variation of plant biomarkers in a plant–soil system. Chemical Geology, 231(3), 190-202.

Cooper, R.J., Pedentchouk, N., Hiscock, K.M., Disdle, P., Krueger, T., Rawlins, B.G. (2015). Apportioning sources of organic matter in streambed sediments: an integrated molecular and compound-specific stable isotope approach. Science of the Total Environment, 520, 187-197.

Cormier, M.A., Werner, R.A., Sauer, P.E., Gröcke, D.R., Leuenberger, M.C., Wieloch, T., ... Kahmen, A. (2018). ^2H-fractionations during the biosynthesis of carbohydrates and lipids imprint a metabolic signal on the δ^2H values of plant organic compounds. New Phytologist, 218(2), 479-491.

Davis, S. M. (1994). Phosphorus inputs and vegetation sensitivity in the Everglades. Everglades: The ecosystem and its restoration, 357-378.

Diefendorf, A.F., Freeman, K.H., Wing, S.L., Graham, H.V. (2011). Production of *n*-alkyl lipids in living plants and implications for the geologic past. Geochimica et Cosmochimica Acta, 75(23), 7472-7485.

Diefendorf, A.F., Freimuth, E.J. (2017). Extracting the most from terrestrial plant-derived *n*-alkyl lipids and their carbon isotopes from the sedimentary record: A review. Organic Geochemistry, 103, 1-21.

Diefendorf, A.F., Mueller, K.E., Wing, S.L., Koch, P.L., Freeman, K.H. (2010). Global patterns in leaf ^{13}C discrimination and implications for studies of past and future climate. Proceedings of the National Academy of Sciences, 107(13), 5738-5743.

Douglas, M.S., (1947) The Everglades river of grass (revised edition, 1988). Pineapple, Sarasota, Florida.

964 Duan, Y., Wu, Y., Cao, X., Zhao, Y., Ma, L. (2014). Hydrogen isotope ratios of
965 individual *n*-alkanes in plants from Gannan Gahai Lake (China) and surrounding
966 area. Organic Geochemistry, 77, 96-105.
967 Dungait, J.A., Docherty, G., Straker, V., Evershed, R.P. (2011). Variation in bulk tissue,
968 fatty acid and monosaccharide $\delta^{13}C$ values between autotrophic and heterotrophic
969 plant organs. Phytochemistry, 72(17), 2130-2138.
970 Eglinton, G., Hamilton, R.J. (1967). Leaf epicuticular waxes. Science, 156(3780), 1322-
971 1335.
972 Eglinton, T.I., Eglinton, G. (2008). Molecular proxies for paleoclimatology. Earth and
973 Planetary Science Letters, 275(1), 1-16.
974 Eley, Y., Dawson, L., Black, S., Andrews, J., Pedentchouk, N. (2014). Understanding
975 $^{2}H/^{1}H$ systematics of leaf wax *n*-alkanes in coastal plants at stiffkey saltmarsh,
976 norfolk, UK. Geochimica et Cosmochimica Acta, 128, 13-28.
977 Ewe, S.M., Sternberg, L.D.S.L. (2003). Seasonal gas exchange characteristics of *Schinus*
978 *terebinthifolius* in a native and disturbed upland community in Everglades National
979 Park, Florida. Forest Ecology and Management, 179(1-3), 27-36.
980 Fahey, T.J., Siccama, T.G., Driscoll, C.T., Likens, G.E., Campbell, J., Johnson, C.E.,
981 Yanai, R.D. (2005). The biogeochemistry of carbon at Hubbard Brook.
982 Biogeochemistry, 75(1), 109-176.
983 Feakins, S.J., Sessions, A.L. (2010). Crassulacean acid metabolism influences D/H ratio
984 of leaf wax in succulent plants. Organic Geochemistry, 41(12), 1269-1276.
985 Feakins, S.J., Wu, M.S., Ponton, C., Galy, V., West, A.J. (2018). Dual isotope evidence
986 for sedimentary integration of plant wax biomarkers across an Andes-Amazon
987 elevation transect. Geochimica et Cosmochimica Acta, 242, 64-81.
988 Ficken, K.J., Li, B., Swain, D.L., Eglinton, G. (2000). An *n*-alkane proxy for the
989 sedimentary input of submerged/floating freshwater aquatic macrophytes. Organic
990 Geochemistry, 31(7), 745-749.
991 Freeman, K.H., Mueller, K.E., Diefendorf, A.F., Wing, S.L., Koch, P.L. (2011).
992 Clarifying the influence of water availability and plant types on carbon isotope
993 discrimination by C3 plants. Proceedings of the National Academy of Sciences,
994 108(16), 59-60.
995 Freeman, K.H., Pancost, R.D., 2014. Biomarkers for Terrestrial Plants and Climate,
996 Treatise on Geochemistry. Second ed. Elsevier, pp. 395-416.
997 Freimuth, E.J., Diefendorf, A.F., Lowell, T.V. (2017). Hydrogen isotopes of *n*-alkanes
998 and *n*-alkanoic acids as tracers of precipitation in a temperate forest and implications
999 for paleorecords. Geochimica et Cosmochimica Acta, 206, 166-183.
1000 Freimuth, E.J., Diefendorf, A.F., Lowell, T.V., Wiles, G.C. (2019). Sedimentary *n*-
1001 alkanes and *n*-alkanoic acids in a temperate bog are biased toward woody plants.
1002 Organic Geochemistry, 128, 94-107.
1003 Gamarra, B., Kahmen, A. (2015). Concentrations and $\delta^{2}H$ values of cuticular *n*-alkanes
1004 vary significantly among plant organs, species and habitats in grasses from an alpine
1005 and a temperate European grassland. Oecologia, 178(4), 981-998.
1006 Gao, L., Edwards, E. J., Zeng, Y., Huang, Y. (2014). Major evolutionary trends in
1007 hydrogen isotope fractionation of vascular plant leaf waxes. PloS One, 9(11).
1008 Gao, L., Hou, J., Toney, J., MacDonald, D., Huang, Y. (2011). Mathematical modeling of
1009 the aquatic macrophyte inputs of mid-chain *n*-alkyl lipids to lake sediments:

implications for interpreting compound specific hydrogen isotopic records. Geochimica et Cosmochimica Acta, 75(13), 3781-3791.
Gao, M., Simoneit, B. R., Gantar, M., Jaffé, R. (2007). Occurrence and distribution of novel botryococcene hydrocarbons in freshwater wetlands of the Florida Everglades. Chemosphere, 70(2), 224-236.
Gill, R.A., Jackson, R.B. (2000). Global patterns of root turnover for terrestrial ecosystems. The New Phytologist, 147(1), 13-31.
Gocke, M., Kuzyakov, Y., Wiesenberg, G.L.B. (2010). Rhizoliths in loess–evidence for post-sedimentary incorporation of root-derived organic matter in terrestrial sediments as assessed from molecular proxies. Organic Geochemistry, 41(11), 1198-1206.
Goslee, S.C., Richardson, C.J. (2008). Establishment and seedling growth of sawgrass and cattail from the Everglades. In Everglades Experiments (pp. 547-564). Springer New York.
Grice, K., Schouten, S., Nissenbaum, A., Charrach, J., Damsté, J.S.S. (1998). A remarkable paradox: sulfurised freshwater algal (Botryococcus braunii) lipids in an ancient hypersaline euxinic ecosystem. Organic Geochemistry, 28(3-4), 195-216.
Grice, K., Schouten, S., Nissenbaum, A., Charrach, J., Damsté, J.S.S. (1998). A remarkable paradox: sulfurised freshwater algal (*Botryococcus braunii*) lipids in an ancient hypersaline euxinic ecosystem. Organic Geochemistry, 28(3-4), 195-216.
Hauke, V., Schreiber, L. (1998). Ontogenetic and seasonal development of wax composition and cuticular transpiration of ivy (*Hedera helix* L.) sun and shade leaves. Planta, 207(1), 67-75.
He, D., Anderson, W.T., Jaffé, R. (2016a). Compound specific δD and $\delta^{13}C$ analyses as a tool for the assessment of hydrological change in a subtropical wetland. Aquatic Sciences, 78(4), 809-822.
He, D., Ladd, S.N., Sachs, J.P., Jaffé, R. (2017). Inverse relationship between salinity and $^{2}H/^{1}H$ fractionation in leaf wax *n*-alkanes from Florida mangroves. Organic Geochemistry, 110, 1-12.
He, D., Mead, R.N., Belicka, L., Pisani, O., Jaffé, R. (2014). Assessing source contributions to particulate organic matter in a subtropical estuary: a biomarker approach. Organic Geochemistry, 75, 129-139.
He, D., Simoneit, B. R., Xu, Y., Jaffé, R. (2016b). Occurrence of unsaturated C_{25} highly branched isoprenoids (HBIs) in a freshwater wetland. Organic Geochemistry, 93, 59-67.
He, D., Simoneit, B.R.T., Jaffé, R. (2018a). Environmental factors controlling the distributions of *Botryococcus braunii* (A, B and L) biomarkers in a subtropical freshwater wetland. Scientific Reports, 8(1).
He, D., Simoneit, B.R.T., Jara, B., Jaffé, R. (2015a). Compositions and isotopic differences of *iso*- and *anteiso*-alkanes in black mangroves (*Avicennia germinans*) across a salinity gradient in a subtropical estuary. Environmental Chemistry, 13, 117-128.
He, D., Simoneit, B.R.T., Jara, B., Jaffé, R. (2015b). Occurrence and distribution of monomethylalkanes in the freshwater wetland ecosystem of the Florida Everglades. Chemosphere, 119, 258-266.

He, D., Zhang, K., Cui, X., Tang, J., Sun, Y. (2018b). Spatiotemporal variability of hydrocarbons in surface sediments from an intensively human-impacted Xiaoqing River-Laizhou Bay system in the eastern China: Occurrence, compositional profile and source apportionment. Science of the Total Environment, 645, 1172-1182.

Hinrichs, K.U., Schneider, R.R., Müller, P.J., Rullkötter, J. (1999). A biomarker perspective on paleoproductivity variations in two Late Quaternary sediment sections from the Southeast Atlantic Ocean. Organic Geochemistry, 30(5), 341-366.

Hobbie, E., Werner, R.A. (2004). Intramolecular, compound-specific, and bulk carbon isotope patterns in C3 and C4 plants: a review and synthesis. New Phytologist, 161(2), 371-385.

Hou, J., D'Andrea, W.J., MacDonald, D., Huang, Y. (2007). Hydrogen isotopic variability in leaf waxes among terrestrial and aquatic plants around Blood Pond, Massachusetts (USA). Organic Geochemistry, 38(6), 977-984.

Huang, X., Wang, C., Zhang, J., Wiesenberg, G.L., Zhang, Z., Xie, S. (2011). Comparison of free lipid compositions between roots and leaves of plants in the Dajiuhu Peatland, central China. Geochemical Journal, 45(5), 365.

Huang, X., Zhao, B., Wang, K., Hu, Y., Meyers, P.A. (2018). Seasonal variations of leaf wax n-alkane molecular composition and δD values in two subtropical deciduous tree species: Results from a three-year monitoring program in central China. Organic Geochemistry, 118, 15-26.

Jaffé, R., Mead, R., Hernandez, M.E., Peralba, M.C., DiGuida, O.A. (2001). Origin and transport of sedimentary organic matter in two subtropical estuaries: a comparative, biomarker-based study. Organic Geochemistry, 32(4), 507-526.

Jansen, B., Nierop, K.G., Hageman, J.A., Cleef, A.M., Verstraten, J.M. (2006). The straight-chain lipid biomarker composition of plant species responsible for the dominant biomass production along two altitudinal transects in the Ecuadorian Andes. Organic Geochemistry, 37(11), 1514-1536.

Jansen, B., Wiesenberg, G.L. (2017). Opportunities and limitations related to the application of plant-derived lipid molecular proxies in soil science. Soil, 3(4), 211.

Jetter, R., Kunst, L., Samuels, A.L. (2006) Biology of the Plant Cuticle, eds Rieder M, Muller C (Blackwell Publishing, Oxford, UK), pp 145-181.

Jimenez, K.L., Starr, G., Staudhammer, C.L., Schedlbauer, J.L., Loescher, H.W., Malone, S.L., Oberbauer, S.F. (2012). Carbon dioxide exchange rates from short-and long-hydroperiod Everglades freshwater marsh. Journal of Geophysical Research: Biogeosciences, 117(G4), doi:10.1029/2012JG002117.

Kahmen, A., Hoffmann, B., Schefuß, E., Arndt, S.K., Cernusak, L.A., West, J.B., et al. (2013). Leaf water deuterium enrichment shapes leaf wax *n*-alkane δD values of angiosperm plants ii: observational evidence and global implications. Geochimica Et Cosmochimica Acta, 111(111), 50-63.

Keough, J.R., Hagley, C.A., Ruzycki, E., Sierszen, M. (1998). $\delta^{13}C$ composition of primary producers and role of detritus in a freshwater coastal ecosystem. Limnology and Oceanography, 43(4), 734-740.

Kohn, M.J. (2010). Carbon isotope compositions of terrestrial C3 plants as indicators of (paleo) ecology and (paleo) climate. Proceedings of the National Academy of Sciences, 107(46), 19691-19695.

Ladd, S.N., Sachs, J.P. (2012). Inverse relationship between salinity and *n*-alkane δD values in the mangrove *Avicennia marina*. Organic Geochemistry, 48, 25-36.
Ladd, S.N., Sachs, J.P. (2015). Influence of salinity on hydrogen isotope fractionation in rhizophora, mangroves from micronesia. Geochimica et Cosmochimica Acta, 168, 206-221.
Ladd, S.N., Sachs, J.P. (2017). $^{2}H/^{1}H$ fractionation in lipids of the mangrove *Bruguiera gymnorhiza* increases with salinity in marine lakes of Palau. Geochimica et Cosmochimica Acta, 204, 300-312.
Li, G., Li, L., Tarozo, R., Longo, W. M., Wang, K. J., Dong, H., Huang, Y. (2018). Microbial production of long-chain *n*-alkanes: Implication for interpreting sedimentary leaf wax signals. Organic Geochemistry, 115, 24-31.
Liu, H., Liu, W. (2016). *n*-Alkane distributions and concentrations in algae, submerged plants and terrestrial plants from the Qinghai-Tibetan Plateau. Organic Geochemistry, 99, 10-22.
Liu, H., Liu, W. (2019). Hydrogen isotope fractionation variations of *n*-alkanes and fatty acids in algae and submerged plants from Tibetan Plateau lakes: Implications for palaeoclimatic reconstruction. Science of The Total Environment, 695, 133925.
Liu, J., An, Z. (2019). Variations in hydrogen isotopic fractionation in higher plants and sediments across different latitudes: Implications for paleohydrological reconstruction. Science of the Total Environment, 650, 470-478.
Liu, J., An, Z., Wu, H., Yu, Y. (2019). Comparison of *n*-alkane concentrations and δD values between leaves and roots in modern plants on the Chinese Loess Plateau. Organic Geochemistry, 138, 103913.
Liu, W., Huang, Y. (2005). Compound specific D/H ratios and molecular distributions of higher plant leaf waxes as novel paleoenvironmental indicators in the Chinese Loess Plateau. Organic Geochemistry, 36(6), 851-860.
Liu, W., Yang, H., Li, L. (2006). Hydrogen isotopic compositions of *n*-alkanes from terrestrial plants correlate with their ecological life forms. Oecologia, 150(2), 330-338.
Malone, S.L., Starr, G., Staudhammer, C.L., Ryan, M.G. (2013). Effects of simulated drought on the carbon balance of Everglades short-hydroperiod marsh. Global Change Biology, 19(8), 2511-2523.
McFarlin, J.M., Axford, Y., Masterson, A.L., Osburn, M.R. (2019). Calibration of modern sedimentary $\delta^{2}H$ plant wax-water relationships in Greenland lakes. Quaternary Science Reviews, 225, 105978.
Mead, R., Xu, Y., Chong, J., Jaffé, R. (2005). Sediment and soil organic matter source assessment as revealed by the molecular distribution and carbon isotopic composition of *n*-alkanes. Organic Geochemistry, 36(3), 363-370.
Mendez-Millan, M., Dignac, M.F., Rumpel, C., Rasse, D.P., Derenne, S. (2010). Molecular dynamics of shoot vs. root biomarkers in an agricultural soil estimated by natural abundance ^{13}C labelling. Soil Biology and Biochemistry, 42(2), 169-177.
Meyers, P.A. (1997). Organic geochemical proxies of paleoceanographic, paleolimnologic, and paleoclimatic processes. Organic Geochemistry, 27(5-6), 213-250.

1144 Nelson, D.B., Ladd, S.N., Schubert, C.J., Kahmen, A. (2018). Rapid atmospheric
1145 transport and large-scale deposition of recently synthesized plant waxes.
1146 Geochimica et Cosmochimica Acta, 222, 599-617.
1147 Nelson, D.B., Sachs, J.P. (2016). Galápagos hydroclimate of the Common Era from
1148 paired microalgal and mangrove biomarker $^{2}H/^{1}H$ values. Proceedings of the
1149 National Academy of Sciences, 113(13), 3476-3481.
1150 Newberry, S. L., Kahmen, A., Dennis, P., Grant, A. (2015). *n*-Alkane biosynthetic
1151 hydrogen isotope fractionation is not constant throughout the growing season in the
1152 riparian tree Salix viminalis. Geochimica et Cosmochimica Acta, 165, 75-85.
1153 Newman, S., Grace, J. B., Koebel, J. W. (1996). Effects of nutrients and hydroperiod on
1154 Typha, Cladium, and Eleocharis: implications for Everglades restoration. Ecological
1155 Applications, 6(3), 774-783.
1156 Oakes, A.M., Hren, M.T. (2016). Temporal variations in the δD of leaf *n*-alkanes from
1157 four riparian plant species. Organic Geochemistry, 97, 122-130.
1158 Pancost, R.D., Boot, C.S. (2004). The palaeoclimatic utility of terrestrial biomarkers in
1159 marine sediments. Marine Chemistry, 92(1-4), 239-261.
1160 Pedentchouk, N., Sumner, W., Tipple, B., Pagani, M. (2008). $\delta^{13}C$ and δD compositions
1161 of *n*-alkanes from modern angiosperms and conifers: An experimental set up in
1162 central Washington State, USA. Organic Geochemistry, 39(8), 1066-1071.
1163 Poret, N., Twilley, R.R., Rivera-Monroy, V.H., and Coronado-Molina, C. (2007).
1164 Belowground decomposition of mangrove roots in Florida Coastal Everglades.
1165 Estuaries and Coasts, 30(3), 491-496.
1166 Price, R.M., Swart, P.K. (2006). Geochemical indicators of groundwater recharge in the
1167 surficial aquifer system: Everglades National Park, Florida, USA. Geological
1168 Society of America Special Papers, 404, 251-266.
1169 Price, R.M., Swart, P.K., Fourqurean, J.W. (2006). Coastal groundwater discharge-an
1170 additional source of phosphorus for the oligotrophic wetlands of the Everglades.
1171 Hydrobiologia, 569(1), 23-36.
1172 Price, R.M., Swart, P.K., Willoughby, H.E. (2008). Seasonal and spatial variation in the
1173 stable isotopic composition ($\delta^{18}O$ and δD) of precipitation in south Florida. Journal
1174 of Hydrology, 358(3), 193-205.
1175 Rasse, D.P., Rumpel, C., Dignac, M.F. (2005). Is soil carbon mostly root carbon?
1176 Mechanisms for a specific stabilisation. Plant and Soil, 269(1-2), 341-356.
1177 Regier, P., He, D., Saunders, C. J., Jara, B., Hansen, C., Newman, S., ...Jaffé, R. (2018).
1178 Sheet Flow Effects on Sediment Transport in a Degraded Ridge-and-Slough
1179 Wetland: Insights Using Molecular Markers. Journal of Geophysical Research:
1180 Biogeosciences, 123(10), 3124-3139.
1181 Ross, M.S., Meeder, J.F., Sah, J.P., Ruiz, P.L., Telesnicki, G.J. (2000). The southeast
1182 saline Everglades revisited: 50 years of coastal vegetation change. Journal of
1183 Vegetation Science, 11(1), 101-112.
1184 Rydin, H., Jeglum, J.K. (2013). The Biology of Peatlands. Oxford university press, New
1185 York.
1186 Sachse, D., Billault, I., Bowen, G.J., Chikaraishi, Y., Dawson, T.E., Feakins, S.J., ... and
1187 Kahmen, A. (2012). Molecular paleo-hydrology: interpreting the hydrogen isotopic
1188 composition of lipid biomarkers from photosynthetic organisms. Annual Review of
1189 Earth Planetary Science, 40, 221-249.

Sachse, D., Gleixner, G., Wilkes, H., Kahmen, A. (2010). Leaf wax *n*-alkane δD values of field-grown barley reflect leaf water δD values at the time of leaf formation. Geochimica et Cosmochimica Acta, 74(23), 6741-6750.

Sachse, D., Radke, J., Gleixner, G. (2004). Hydrogen isotope ratios of recent lacustrine sedimentary *n*-alkanes record modern climate variability. Geochimica et Cosmochimica Acta, 68(23), 4877-4889.

Sachse, D., Radke, J., Gleixner, G. (2006). δD values of individual *n*-alkanes from terrestrial plants along a climatic gradient–Implications for the sedimentary biomarker record. Organic Geochemistry, 37(4), 469-483.

Saha, A.K., Sternberg, L.O.R., da Silviera, L., Miralles-Wilhelm, F. (2009). Linking water sources with foliar nutrient status in upland plant communities in the Everglades National Park, USA. Ecohydrology, 2(1), 42-54.

Saunders, C.J., Gao, M., Jaffé, R. (2015). Environmental assessment of vegetation and hydrological conditions in Everglades freshwater marshes using multiple geochemical proxies. Aquatic Sciences, 77(2), 271-291.

Saunders, C.J., Gao, M., Lynch, J.A., Jaffé, R., Childers, D.L. (2006). Using soil profiles of seeds and molecular markers as proxies for sawgrass and wet prairie slough vegetation in Shark Slough, Everglades National Park. Hydrobiologia, 569(1), 475-492.

Seki, O., Nakatsuka, T., Shibata, H., Kawamura, K. (2010). A compound-specific n-alkane $\delta^{13}C$ and δD approach for assessing source and delivery processes of terrestrial organic matter within a forested watershed in northern Japan. Geochimica et Cosmochimica Acta, 74(2), 599-613.

Sessions, A.L. (2016). Factors controlling the deuterium contents of sedimentary hydrocarbons. Organic Geochemistry, 96, 43-64.

Simoneit, B.R. (1977). Biogenic lipids in particulates from the lower atmosphere over the eastern Atlantic. Nature, 267, 682-685.

Spooner, N., Rieley, G., Collister, J.W., Lander, M., Cranwell, P.A., Maxwell, J.R. (1994). Stable carbon isotopic correlation of individual biolipids in aquatic organisms and a lake bottom sediment. Organic Geochemistry, 21(6-7), 823-827.

Sternberg, L., Deniro, M.J., Ajie, H. (1984). Stable hydrogen isotope ratios of saponifiable lipids and cellulose nitrate from CAM, C_3 and C_4 plants. Phytochemistry, 23(11), 2475-2477.

Sternberg, L.S., Swart, P.K., 1987. Utilization of freshwater and ocean water by coastal plants of southern Florida. Ecology, 68, 1898-1905.

Taylor, A.K., Benedetti, M.M., Haws, J.A., Lane, C.S. (2019). The hydrogen isotopic compositions of sedimentary mid-chain n-alkanes record ecological change at a Portuguese paleowetland. Quaternary International, 532, 23-33.

Tierney, J.E., Russell, J.M., Huang, Y., Damsté, J.S.S., Hopmans, E.C., Cohen, A.S. (2008). Northern hemisphere controls on tropical southeast African climate during the past 60,000 years. Science, 322(5899), 252-255.

Tipple, B.J., Berke, M.A., Doman, C.E., Khachaturyan, S., Ehleringer, J.R. (2013). Leaf-wax *n*-alkanes record the plant–water environment at leaf flush. Proceedings of the National Academy of Sciences, 110(7), 2659-2664.

Tipple, B.J., Ehleringer, J.R. (2018). Distinctions in heterotrophic and autotrophic-based metabolism as recorded in the hydrogen and carbon isotope ratios of normal alkanes. Oecologia, 187(4), 1053-1075.

Tu, T.N., Derenne, S., Largeau, C., Bardoux, G., Mariotti, A. (2004). Diagenesis effects on specific carbon isotope composition of plant *n*-alkanes. Organic Geochemistry, 35(3), 317-329.

Wang, G., Zhang, L., Zhang, X., Wang, Y., Xu, Y. (2014). Chemical and carbon isotopic dynamics of grass organic matter during litter decompositions: A litterbag experiment. Organic Geochemistry, 69, 106-113.

Wiesenberg, G.L., Gocke, M., Kuzyakov, Y. (2010). Fast incorporation of root-derived lipids and fatty acids into soil–Evidence from a short term multiple $^{14}CO_2$ pulse labelling experiment. Organic Geochemistry, 41(9), 1049-1055.

Xie, S., Nott, C.J., Avsejs, L.A., Volders, F., Maddy, D., Chambers, F.M., ... Evershed, R. P. (2000). Palaeoclimate records in compound-specific δD values of a lipid biomarker in ombrotrophic peat. Organic Geochemistry, 31(10), 1053-1057.

Ziegler, H., Osmond, C.B., Stichler, W., Trimborn, P. (1976). Hydrogen isotope discrimination in higher plants: Correlations with photosynthetic pathway and environment. Planta, 128, 85-92.

Figure and Table captions

Figure 1: Map showing the study area: (a) study sites across the Everglades, (b) the transition from tress island/freshwater wetland to mangrove estuary and then to Florida Bay (modified from Lodge, 1994), (c) and (d) mosaic of the tree island-freshwater wetland ridge and slough landscape. Note: GL tree island is a tree island site, WCA3, SRS1-3 and TSPh2 are freshwater wetland sites, SRS4-6 are mangrove estuarine sites with mesohaline water, Florida Bay is a pure marine water site. The detailed hydrological parameters of each site is detailed in Table S1.

Figure 2: *n*-Alkane distributions and their δ^2H and $\delta^{13}C$ values across studied plant leaves. Note: all the δ^2H and $\delta^{13}C$ values are CWA of odd numbered *n*-alkanes (*n*-C_{23} to *n*-C_{33}); n.d. denotes no data.

Figure 3: *n*-Alkane distributions and CWA δ^2H and $\delta^{13}C$ values in leaves of the typical Everglades plants classified by plant functional types. TI: tree island plants, EW: emergent wetland plants; SW: submerged wetland plants; MA: mangroves; MS: marine seagrass plants; Sediments: surface sediments from SRS2. The "n" in each panel denotes number of species surveyed.

Figure 4: *n*-Alkane distributions and average δ^2H and $\delta^{13}C$ values in leaves and roots among the typical Everglades freshwater wetland plants.

Figure 5: Principal component analysis of all Everglades plants (leaves and roots), one slough core and one ridge core soil samples (from SRS2). Note: b) and d), TI, terrestrial island plants, EW, emergent wetland plants, SW, wetland submerged plants, MA, mangroves, MS, marine seagrass, EWR, emergent wetland plant root, SWR, submerged wetland plant root, Ridge, ridge core sediments, Slough, slough core sediments. The data of slough and ridge core was reorganized from He et al. (2016a). Note: the "*n*-alkane" loading in Fig. 5a,c denotes concentrations of total *n*-alkanes from *n*-C_{23} to *n*-C_{33}.

Table 1: Sampling information of plants from the Florida Everglades. Note: a, both above ground (leaf or stem) and below ground (root) biomass was sampled, X + X in column "Sample Number" denotes for X (Plant leaves or stems) + X (Plant roots); for all the other plant species, only leaves were sampled; b Sargassum is a genus and the exact

species is not identified; c, the percent coverage data is obtained from Todd et al. (2010); d, for the plant functional type, TI, EW, SW, MA and MS denote terrestrial island plants, freshwater wetland emergent plants, freshwater wetland submerged (or floating) plants, estuarine mangroves and marine seagrass, respectively. The plants were also classified by phylum or class, or major taxonomic group (presented by Figs. S7 and S8). Due to the spatial gradient of growing habitat and water source (freshwater to marine water), we preferred to group the plants stated above. N.D. denotes no data.

Table 2: *n*-Alkane concentrations, P*aq*, ACL, CPI and CWA *n*-alkane δ^2H and $\delta^{13}C$ values across studied plants (leaf) across the Florida Everglades. Note: n (SD) means "number of separate samples (standard deviation)".

Table 3: *n*-Alkane concentrations, P*aq*, ACL, CPI and CWA *n*-alkane δ^2H and $\delta^{13}C$ values across studied plants (root) within the freshwater wetland of the Florida Everglades.

Species	Percent coverage [c]	Phylum or Class	Major taxonomic group	Sampling time	Sampling Locations	Plant type [d]	Sample number
Blechnum chilense	N.D.	Fern	Forb	May 2011	GL tree island	TI	2
Osmunda regalis	N.D.	Fern	Forb	May 2011	GL tree island	TI	2
Taxodium distichum	1.5	Gymnosperms	Tree	May 2011	GL tree island	TI	1
Pinus elliottii	N.D.	Gymnosperms	Tree	May 2011	GL tree island	TI	1
Magnolia virginiana	N.D.	Eudicots	Tree	May 2011	GL tree island	TI	3
Persea borbonia	N.D.	Eudicots	Tree	May 2011	GL tree island	TI	1
Chrysobalanus icaco	N.D.	Eudicots	Tree	May 2011	GL tree island	TI	1
Annona glabra	N.D.	Eudicots	Shrub	May 2011	GL tree island	TI	6
Myrica cerifera	N.D.	Eudicots	Shrub	May 2011	GL tree island	TI	3
Salix Caroliniana	1.5	Eudicots	Shrub	May 2011	GL tree island	TI	3
Cephalanthus occidentalis	N.D.	Eudicots	Shrub	May 2011	GL tree island	TI	3
Typha latifolia [a]	1.1	Monocots	Forb	May 2011; Mar. 2013	WCA3, SRS2, TSPh2	EW	3+3
Typha domingensis [a]		Monocots	Forb	May 2011; Mar. 2013	WCA3	EW	6+4
Cladium jamaicense [a]	60.7	Monocots	Forb	May 2011; Mar. 2013	WCA3, SRS2, TSPh2	EW	20+9
Eleocharis cellulosa [a]	3	Monocots	Forb	May 2011; Mar. 2013	WCA3, SRS2, TSPh2	EW	9+4
Eleocharis elongata [a]		Monocots	Forb	Mar. 2013	WCA3	EW	1+1
Nymphaeaceae sp. [a]	N.D.	Eudicots	Forb	May 2011; Mar. 2013	WCA3, SRS2, TSPh2	SW	8+6
Utricularia foliosa	N.D.	Eudicots	Forb	May 2011; Mar. 2013	WCA3, SRS2, TSPh2	SW	9
Utricularia purpurea	N.D.	Eudicots	Forb	May 2011; Mar. 2013	WCA3	SW	3
Bacopa caroliniana	N.D.	Eudicots	Forb	Mar. 2013	WCA3	SW	2
Chara spp.	N.D.	Charophyta	Algae	Mar. 2013	WCA3	SW	1
Rhizophora mangle	2.2	Eudicots	Tree	Mar. 2013	SRS4-6	MA	14
Laguncularia racemosa	N.D.	Eudicots	Tree	Mar. 2013	SRS4-6	MA	10

Avicennia germinans	N.D.	Eudicots	Tree	Mar. 2013	SRS5-6	MA	7
Syringodium filiforme	N.D.	Monocots	Forb	Aug. 2004	Florida Bay	MS	2
Ruppia maritima L.	N.D.	Monocots	Forb	Aug. 2004	Florida Bay	MS	1
Halodule wrightii	N.D.	Eudicots	Forb	Aug. 2004	Florida Bay	MS	1
Halophila decipiens	N.D.	Eudicots	Forb	Aug. 2004	Florida Bay	MS	1
Sargassum [b]	N.D.	Phaeophyceae	Algae	Aug. 2004	Florida Bay	MS	1
Caulerpa spp.	N.D.	Chlorophyta	Algae	Aug. 2004	Florida Bay	MS	1

Table 1

Species (leaves)	*n*-Alkanes (μg/gdw)	n (SD)	P*aq*	n (SD)	ACL	n (SD)	CPI	n (SD)	$\delta^{13}C$	n (SD)	$\delta^{2}H$	n (SD)
Blechnum chilense	3.6	1	0.05	1	28.25	1	7.08	1	-31.5	1	-89	1
Osmunda regalis	63.1	1	0.05	1	28.63	1	6.15	1	-32.7	1	-86	1
Taxodium distichum	6.7	1	0.17	1	28.83	1	4.07	1	-29.1	1	-95	1
Pinus elliottii	8.2	1	0.2	1	29.21	1	3.01	1	-32	1	-91	1
Magnolia virginiana	241.6	3 (92.3)	0.12	2 (0.02)	28.04	3 (0.21)	5.47	3 (1.85)	-34.8	3 (1.5)	-86	3 (3)
Persea borbonia	29.6	1	0.21	1	28.27	1	10.75	1	-33.4	1	-78	1
Chrysobalanus icaco	473.2	1	0	1	29.72	1	9.52	1	-37.8	1	-79	1
Annona glabra	88.3	6 (72.0)	0.09	6 (0.07)	28.49	6 (0.75)	5.35	6 (2.16)	-33.3	3 (1.1)	-85	3 (3)
Myrica cerifera	63.2	3 (20.9)	0.003	3 (0.00)	30.73	3 (0.07)	14.08	3 (1.30)	-33.4	2	-93	2
Salix Caroliniana	214	3 (114.5)	0.1	3 (0.07)	28.26	3 (0.40)	21.61	3 (5.67)	-32.2	3 (1.87)	-89	3 (2)
Cephalanthus occidentalis	281	1	0.01	1	29.44	1	19.57	1	-31.4	1	-91	1
Typha latifolia	153	3 (62.1)	0.13	3 (0.05)	28.13	3 (0.29)	5.59	3 (1.74)	-36.2	3 (0.4)	-128	3 (5)
Typha domingensis	20.6	5 (7.7)	0.21	5 (0.10)	27.85	5 (0.22)	6.49	5 (3.13)	-33.6	5 (0.3)	-137	4 (8)
Cladium jamaicense	256.2	20 (175.0)	0.26	20 (0.14)	27.55	20 (0.36)	6.86	20 (2.90)	-32.2	10 (1.5)	-231	10 (24)
Eleocharis cellulosa	27.8	7 (11.9)	0.32	7 (0.24)	28.20	7 (1.87)	15.05	7 (11.8)	-34.7	7 (1.2)	-115	5 (8)
Eleocharis elongata	25.1	1	0.65	1	26.41	1	10.72	1	-34.2	1	-137	1

Nymphaeaceae sp.	100.4	6 (57.8)	0.55	6 (0.16)	26.32	6 (0.42)	45.56	6 (16.2)	-32.2	6 (1.0)	-118	6 (9)
Utricularia foliosa	86	9 (54.7)	0.75	9 (0.14)	25.93	9 (0.64)	30.77	9 (21.8)	-38.7	8 (1.1)	-119	8 (10)
Utricularia purpurea	114.1	3 (6.5)	0.78	3 (0.05)	25.72	3 (0.36)	53.53	3 (36.2)	-35.8	3 (0.7)	-123	3 (5)
Bacopa caroliniana	72.8	2	0.5	2	28.09	2	4.66	2	-31.1	2	-124	2
Chara sp.	2.4	1	0.8	1	24.96	1	14.34	1	-25.1	1		
Rhizophora mangle	63.4	14 (16.9)	0.08	14 (0.05)	29.13	14 (0.25)	6.50	14 (0.81)	-38.9	14 (1.1)	-131	14 (5)
Laguncularia racemosa	104.8	10 (40.4)	0.08	10 (0.02)	28.28	10 (0.20)	7.56	10 (0.85)	-37.3	10 (1.3)	-141	10 (1)
Avicennia germinans	77.2	7 (10.8)	0.23	7 (0.04)	29.13	7 (0.14)	5.82	7 (0.43)	-36.4	7 (0.9)	-174	3 (5)
Syringodium filiforme	62.9	2	0.92	2	23.94	2	36.25	2	-14.8	2	-86	2
Ruppia maritima L.	63.5	1	0.75	1	25.71	1	27.18	1	-17.1	1	-84	1
Halodule wrightii	375.1	1	0.95	1	24.71	1	40.02	1	-14.4	1	-92	1
Halophila decipiens	2.1	1	0.95	1	24.57	2	N.A.	N.A.	-17.3	1	N.D.	N.D.
Sargassum [b]	4.9	1	0.96	1	24.00	1	3.60	1	N.D.	N.D.	N.D.	N.D.
Caulerpa spp.	7.6	1	0.88	1	24.93	1	1.91	1	N.D.	N.D.	N.D.	N.D.

Table 2

Note: N.A. denotes not applicable, N.D., no data.

Species (Roots)	*n*-Alk. (μg/g dw) (n, SD)	Diff.	P*aq* (n, SD)	Diff.	ACL (n, SD)	Diff.	CPI (n, SD)	Diff.	$\delta^{13}C$ (n, SD)	Diff.	$\delta^{2}H$ (n, SD)	Diff.
T. latifolia	39.5 (3, 21.4)	-113.5	0.59 (3, 0.12)	0.46	26.43 (3, 0.60)	-1.70	24.03 (3, 8.79)	18.44	-33.8 (3, 4.5)	2.4	-133 (3, 4)	-5
T. domingensis	6.9 (4, 3.2)	-13.7	0.47 (4, 0.1)	0.26	26.85 (4, 0.39)	-1.00	11.18 (4, 4.94)	4.69	-34.1 (4, 0.5)	-0.5	-129 (4, 2)	8
C. jamaicense	91.8 (9, 80.3)	-164.4	0.48 (9, 0.15)	0.22	26.95 (9, 0.55)	-0.60	18.48 (9, 16.4)	11.62	-31.1 (6, 1.2)	1.1	-206 (6, 10)	25
E. cellulosa	141.5 (4, 98.2)	113.7	0.94 (4, 0.01)	0.62	25.02 (4, 0.17)	-3.18	42.76 (4, 8.35)	27.71	-32.8 (3, 1.9)	1.9	-133 (3, 3)	-18
E. elongata	102.2 (1, N.A.)	77.1	0.94 (1, N.A.)	0.29	25.03 (1, N.A.)	-1.38	36.67 (1, N.A.)	16.99	-33.5 (1, N.A.)	0.7	-134 (1, N.A.)	3
Nymphaeaceae sp.	87.9 (6, 50.8)	-12.5	0.76 (6, 0.15)	0.21	25.51 (6, 0.87)	-0.81	27.05 (6, 18.80)	-18.51	-30.6 (6, 0.3)	1.6	-131 (3, 6)	13

Table 3

Note: *n*-Alk. stands for *n*-Alkanes; SD, standard deviation; N.A., not applicable; Diff., the value difference between roots and their leaf counter parts (values of roots minus values of leaves).

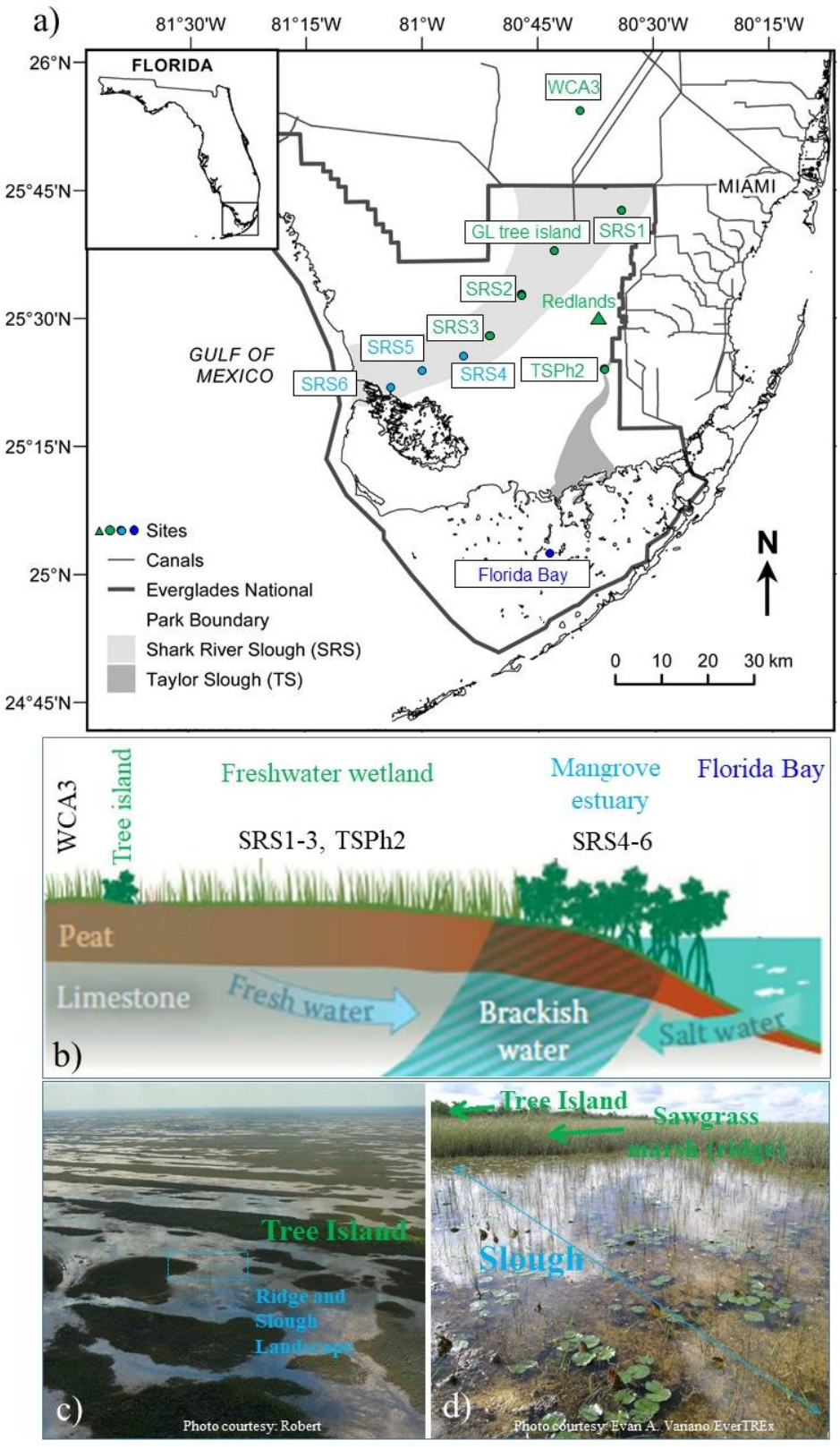
a)
81°30'W
81°15'W
81°W
80°45'W
80°30'W
80°15'W
26°N
25°45'N
25°30'N
25°15'N
25°N
24°45'N
FLORIDA
WCA3
MIAMI
GL tree island
SRS1
SRS2
Redlands
SRS3
SRS5
SRS4
TSPh2
SRS6
GULF OF MEXICO
Florida Bay
Sites
Canals
Everglades National Park Boundary
Shark River Slough (SRS)
Taylor Slough (TS)
N
0 10 20 30 km
WCA3
Tree island
Freshwater wetland
SRS1-3, TSPh2
Mangrove estuary
SRS4-6
Florida Bay
Peat
Limestone
Fresh water
Brackish water
Salt water
b)
Tree Island
Ridge and Slough Landscape
c)
Photo courtesy: Robert
Tree Island
Sawgrass marsh (ridge)
Slough
d)
Photo courtesy: Evan A. Vanano/EverTREx

Fig. 1

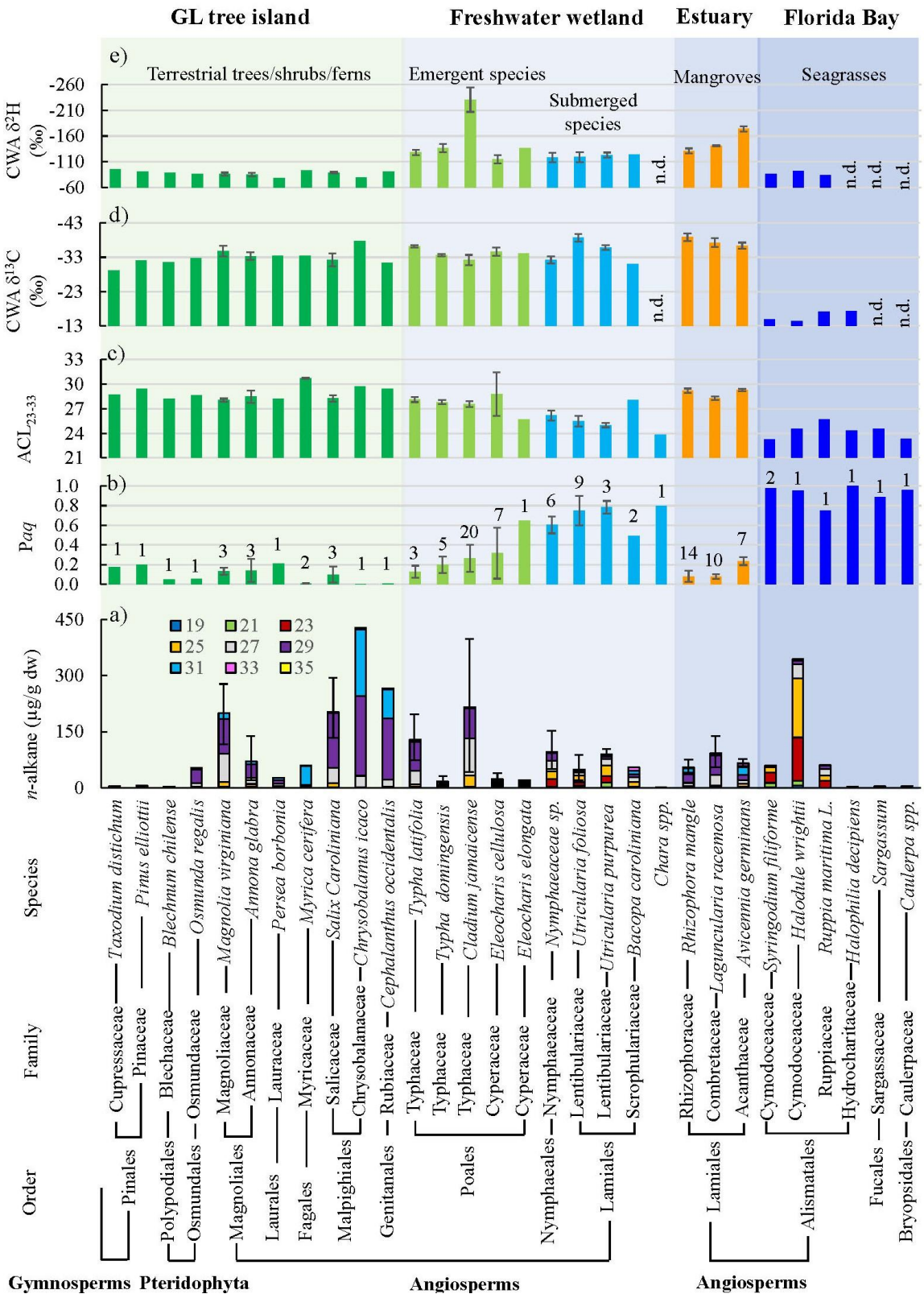
GL tree island
Freshwater wetland
Estuary
Florida Bay
e)
Terrestrial trees/shrubs/ferns
Emergent species
Submerged species
Mangroves
Seagrasses
CWA δ2H (‰)
d)
CWA δ13C (‰)
c)
ACL23-33
b)
Paq
a)
n-alkane (μg/g dw)
19 21 23 25 27 29 31 33 35
n.d.
Order
Family
Species
Taxodium distichum
Pinus elliottii
Blechum chilense
Osmunda regalis
Magnolia virginiana
Annona glabra
Persea borbonia
Myrica cerifera
Salix Caroliniana
Chrysobalanus icaco
Cephalanthus occidentalis
Typha latifolia
Typha domingensis
Cladium jamaicense
Eleocharis cellulosa
Eleocharis elongata
Nymphaeaceae sp.
Utricularia foliosa
Utricularia purpurea
Bacopa caroliniana
Chara spp.
Rhizophora mangle
Laguncularia racemosa
Avicennia germinans
Syringodium filiforme
Halodule wrightii
Ruppia maritima L.
Halophilia decipiens
Sargassum
Caulerpa spp.
Pinales
Polypodiales
Osmundales
Magnoliales
Laurales
Fagales
Malpighiales
Genitanales
Poales
Nymphaeales
Lamiales
Alismatales
Fucales
Bryopsidales
Cupressaceae
Pinaceae
Blechaceae
Osmundaceae
Magnoliaceae
Annonaceae
Lauraceae
Myricaceae
Salicaceae
Chrysobalanaceae
Rubiaceae
Typhaceae
Cyperaceae
Nymphaeaceae
Lentibulariaceae
Scrophulariaceae
Rhizophoraceae
Combretaceae
Acanthaceae
Cymodoceaceae
Ruppiaceae
Hydrocharitaceae
Sargassaceae
Caulerpaceae
Gymnosperms
Pteridophyta
Angiosperms
Angiosperms

Fig. 2

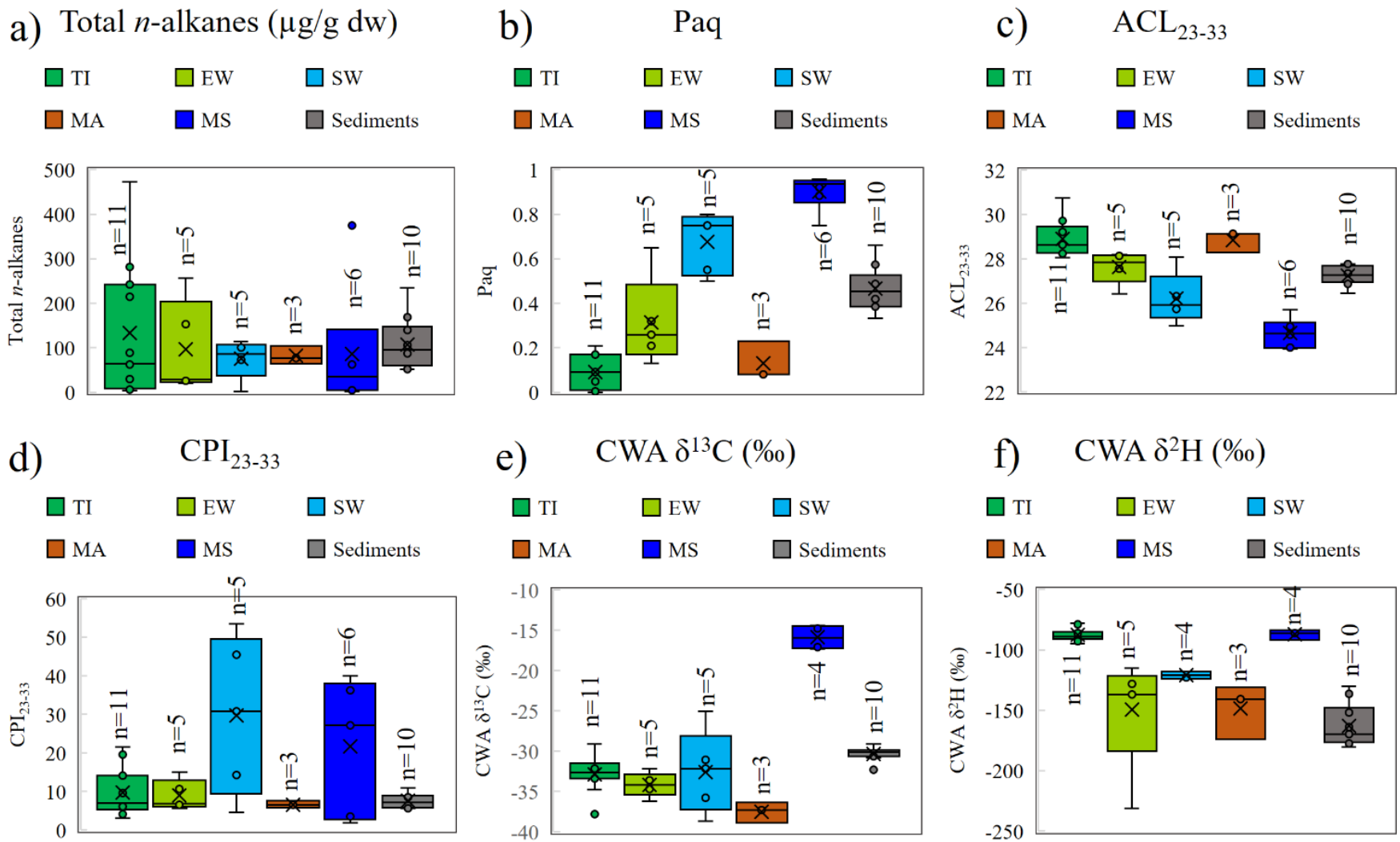
a) Total n-alkanes (µg/g dw)
b) Paq
c) ACL23-33
d) CPI23-33
e) CWA δ13C (‰)
f) CWA δ2H (‰)
TI
EW
SW
MA
MS
Sediments
Total n-alkanes
Paq
ACL23-33
CPI23-33
CWA δ13C (‰)
CWA δ2H (‰)
n=11
n=5
n=3
n=6
n=10
n=4

Fig. 3

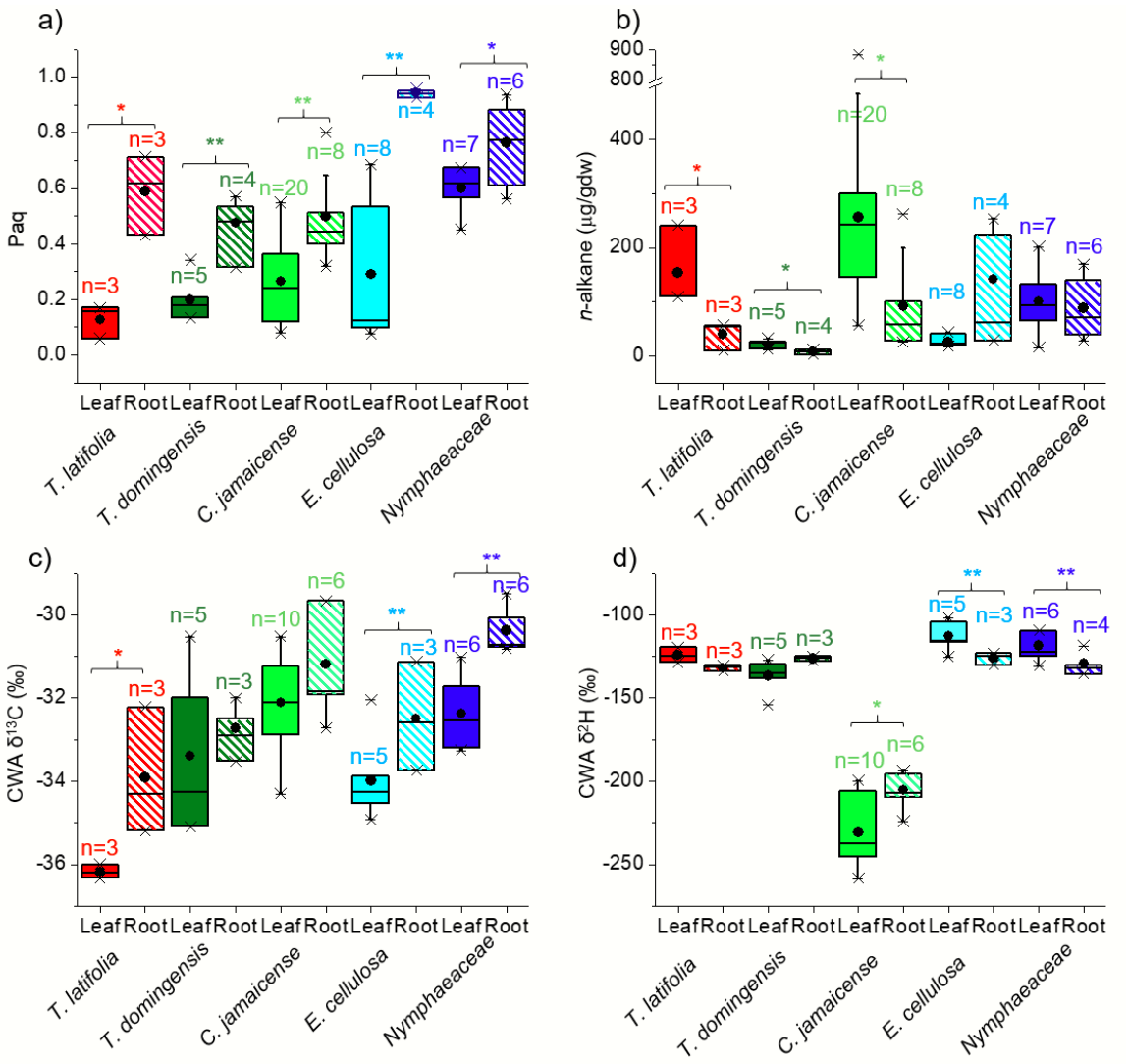
a)
Paq
1.0
0.8
0.6
0.4
0.2
0.0
n=3
n=3
n=5
n=4
n=20
n=8
n=8
n=7
n=4
n=6
Leaf Root Leaf Root Leaf Root Leaf Root Leaf Root
T. latifolia
T. domingensis
C. jamaicense
E. cellulosa
Nymphaeaceae
b)
n-alkane (µg/gdw)
900
800
400
200
0
n=3
n=3
n=5
n=4
n=20
n=8
n=8
n=4
n=7
n=6
Leaf Root Leaf Root Leaf Root Leaf Root Leaf Root
T. latifolia
T. domingensis
C. jamaicense
E. cellulosa
Nymphaeaceae
c)
CWA δ13C (‰)
-30
-32
-34
-36
n=3
n=3
n=5
n=3
n=10
n=6
n=5
n=3
n=6
n=6
Leaf Root Leaf Root Leaf Root Leaf Root Leaf Root
T. latifolia
T. domingensis
C. jamaicense
E. cellulosa
Nymphaeaceae
d)
CWA δ2H (‰)
-100
-150
-200
-250
n=3
n=3
n=5
n=3
n=10
n=6
n=5
n=3
n=6
n=4
Leaf Root Leaf Root Leaf Root Leaf Root Leaf Root
T. latifolia
T. domingensis
C. jamaicense
E. cellulosa
Nymphaeaceae

Fig. 4

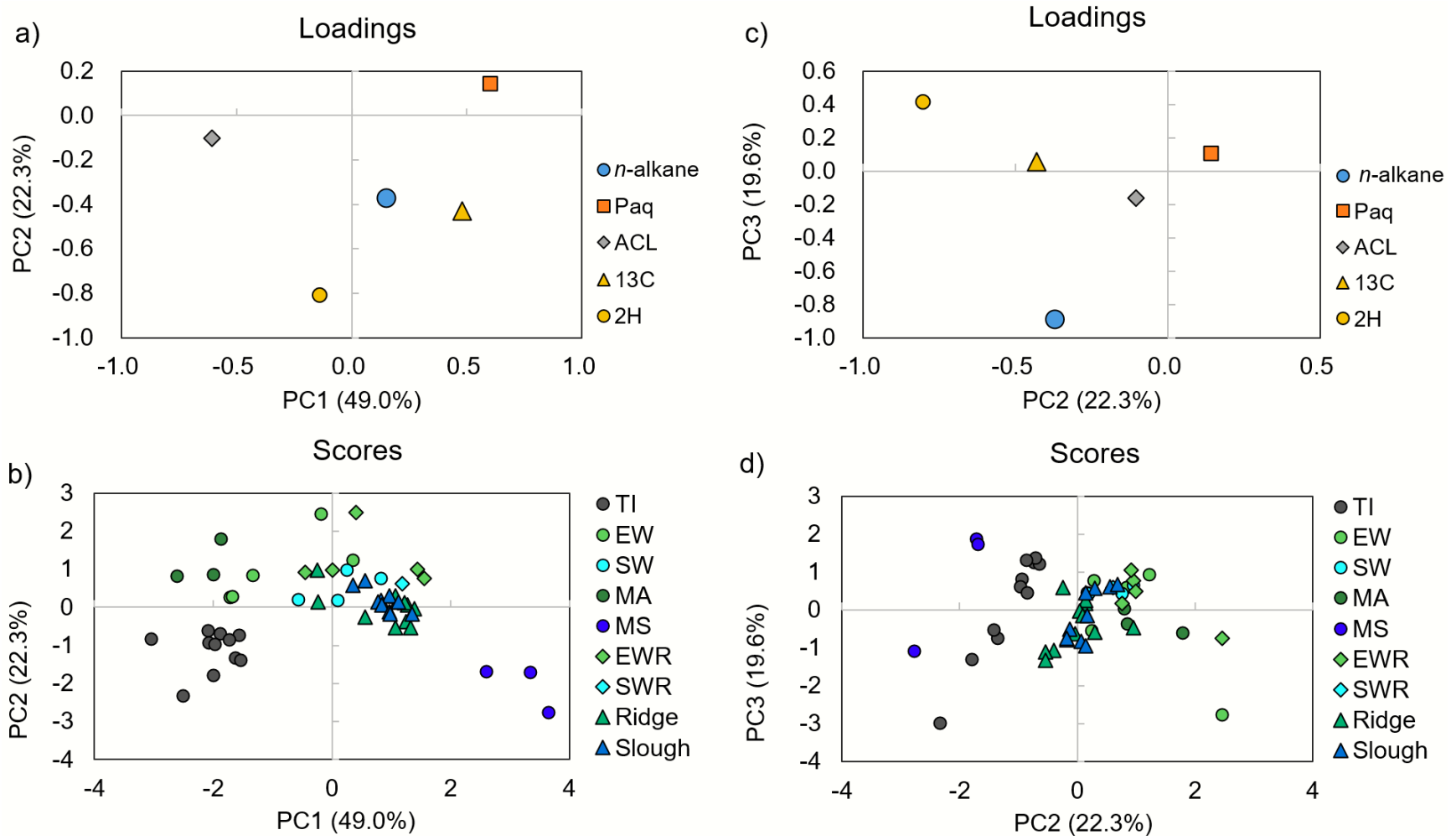
a)
Loadings
PC2 (22.3%)
PC1 (49.0%)
n-alkane
Paq
ACL
13C
2H
c)
Loadings
PC3 (19.6%)
PC2 (22.3%)
n-alkane
Paq
ACL
13C
2H
b)
Scores
PC2 (22.3%)
PC1 (49.0%)
TI
EW
SW
MA
MS
EWR
SWR
Ridge
Slough
d)
Scores
PC3 (19.6%)
PC2 (22.3%)
TI
EW
SW
MA
MS
EWR
SWR
Ridge
Slough

Fig. 5